

A COMPARISON OF THE BEHAVIOUR OF REINFORCED CONCRETE BEAM-COLUMN JOINTS DESIGNED FOR DUCTILITY AND LIMITED DUCTILITY

by R. Park¹ and Dai Ruitong²

ABSTRACT

Four beam-interior column Units were designed, constructed and tested subjected to simulated earthquake and gravity loading. One Unit followed the requirements of the New Zealand concrete design code NZS 3101:1982 for structures designed for ductility. The other three Units only partly followed the requirements of NZS 3101, in order to obtain information on the behaviour of beam-column joints of limited ductility. Plastic hinging was designed to occur in the beams. The major test variables were the quantity of horizontal and vertical shear reinforcement in the beam-interior column joint cores and the diameter of the beam longitudinal reinforcing bars passing through the joint cores. The test results indicated that the current NZS 3101 detailing requirements for shear and bond in the beam-interior column joint core regions of ductile reinforced concrete frames could be relaxed.

NOTATION

| | | | |
|----------|---|-----------|---|
| A_g | area of gross section of column | h_c | column depth parallel to the longitudinal beam bars being considered |
| A_s | area of tension reinforcement of beam | K | a constant |
| A'_s | area of compression reinforcement of beam | L | length of beam of test Unit |
| A_{st} | total area of reinforcement in column | M_{1u} | positive moment flexural strength of beam calculated using the code approach |
| b_w | beam width | M_{2u} | negative moment flexural strength of beam calculated using the code approach |
| d_b | reinforcing bar diameter | P_e | axial compression load on column |
| E_s | modulus of elasticity of steel | P | gravity load on beam |
| E_{sh} | strain-hardening modulus of steel | u_b | bond stress between longitudinal bars and concrete |
| f'_c | compressive cylinder strength of concrete | V_{ch} | ideal horizontal joint shear strength provided by concrete shear resisting mechanism only |
| f_{su} | ultimate tensile strength of steel | V_{cv} | ideal vertical joint shear strength provided by concrete shear resisting mechanism only |
| f_y | yield strength of longitudinal reinforcing steel | V_c | ideal shear force resisted by concrete shear resisting mechanisms |
| f_{yh} | yield strength of transverse reinforcing steel | V_{jh} | total horizontal shear force across a joint |
| H | overall height of column of Unit = storey height of frame | V_{jv} | total vertical shear force across a joint |
| h_b | beam depth | V_{max} | maximum experimental horizontal load |

¹ Professor and Head of Civil Engineering, University of Canterbury, New Zealand.
² Lecturer, Branch College of Tongji University, Shanghai, China.

| | |
|-----------------|---|
| V_{sh} | ideal horizontal joint shear strength provided by horizontal joint shear reinforcement |
| V_{sv} | ideal vertical joint shear strength provided by vertical joint shear reinforcement |
| V_1 | horizontal load at column top of test Unit when first plastic hinge forms in beam |
| V_2 | horizontal load at column top of test Unit when both plastic hinges (first plastic hinge and second plastic hinge) form in beam |
| yL | distance from gravity load point to face of column |
| α | beam longitudinal steel overstrength factor |
| β | A'_s/A_s |
| Δ | horizontal displacement of column top |
| Δ_y | first yield displacement in experiment |
| Δ_{y1} | horizontal displacement at column top along pushing direction at three-quarters of theoretical horizontal ultimate load |
| Δ_{y2} | horizontal displacement at column top along pulling direction at three-quarters of theoretical horizontal ultimate load |
| ϵ_{sf} | steel strain at fracture |
| ϵ_{sh} | steel strain at the commencement of strain hardening |
| ϵ_y | steel strain at first yield |
| ϕ | strength reduction factor |
| μ | displacement ductility factor |
| ρ | ratio of tension reinforcement in a beam = $A_s/b_w d$ |
| ρ' | ratio of compression reinforcement in a beam = $A'_s/b_w d$ |
| ρ_t | ratio of total reinforcement in a column = A_{st}/A_g |

1. INTRODUCTION

According to the current New Zealand design codes (1,2), reinforced concrete structures can be designed to resist major earthquakes either as "ductile structures" or as "structures of limited ductility".

Ductile structures are designed in New Zealand using the capacity design procedure (1,2). This design procedure can be relatively complex and results in significant quantities of transverse reinforcement in members and beam-column

joints in order to confine the compressed concrete, to prevent premature buckling of the longitudinal reinforcement, and to provide shear resistance.

As an alternative, some structures, particularly frames or walls of small buildings, may be designed to withstand higher seismic design loads and hence would need only limited ductility. That is, the level of seismic design load used could be part way between the level for a ductile structure and that for an elastically responding structure. The advantage of the design procedure for limited ductility is that a capacity design procedure is then unnecessary, a considerable relaxation in the detailing requirements for ductility is permitted, and the design is less complex.

The New Zealand code for general structural design and design loadings for buildings, NZS 4203:1984 (1) currently permits a limited ductility design approach for moment resisting frames up to 4 or 5 storeys maximum height. The design seismic loading specified for frames of limited ductility is 2.5 times that used for ductile frames. The New Zealand code for the design of concrete structures, NZS 3101:1982(2) has a Chapter 14 which gives seismic design provisions for structures of limited ductility designed for that code seismic loading.

It is of note that the design provisions for limited ductility of Chapter 14 of NZS 3101 are in need of expansion and that they are based on sparse test evidence of the behaviour of reinforced concrete moment resisting frames of limited ductility. The need for expansion of Chapter 14 has recently become more pressing. A proposed draft replacement for NZS 4203 (3), circulated for comment in 1986, has moved a stage further in permitting the designer to select a structure ductility factor anywhere in the wide range of between 1.25 for an elastically responding frame and 6 for a ductile frame, and to design the structure for the seismic design load and section ductility corresponding to that chosen structure ductility factor. Hence more detailed rules for the design of reinforced concrete structures for limited ductility are needed. A recent report of a Study Group of the New Zealand National Society for Earthquake Engineering for structures of limited ductility (4) gives an outline of current New Zealand code provisions for structures of limited ductility.

Experience has shown that beam-column joints can be the critical regions in reinforced concrete frames subjected to severe earthquake loading. The Department of Civil Engineering of the University of Canterbury has conducted research into the behaviour of reinforced concrete beam-column joints under simulated seismic loading since the early 1970's. That work, summarised in Refs. 5, 6 and 7, has led to the requirements for transverse reinforcement in the joints of ductile frames specified by the New Zealand concrete design code NZS 3101:1982 (2).

Less research has been conducted into the detailing requirements for frames where the seismic design loadings are such that limited ductility would be adequate in order to survive a major earthquake. The design rules for beam-column joints of frames of limited ductility in NZS 3101:1982 are not so specific.

The aim of this study was to further investigate the bond strength and shear resisting mechanisms in beam-interior column joint cores with the aim of obtaining additional information on the behaviour of reinforced concrete joints of ductile frames and of frames of limited ductility. The results of the study may be seen reported in more detail elsewhere (8).

2. DESIGN OF THE BEAM-INTERIOR COLUMN JOINT UNITS

2.1 Dimensions and Loading

The deflected shape of a moment resisting plane frame resulting from lateral earthquake loading and gravity loading is shown in Fig. 1. Figure 2 shows a subassemblage of the frame with loading as used in this study to investigate the behaviour of interior beam-column joint regions. The ends of the members of the subassemblage coincide with the mid-span and mid-height points of the frame. When lateral loads are applied to the ends of the column the subassemblage is displaced horizontally, but the ends of the beams are prevented from displacing vertically. Vertical loads are also applied to the beams. The applied column axial load was zero in the tests in order to give the worse loading case for the beam-column joint core.

The overall dimensions of the four beam-column units tested in this study,

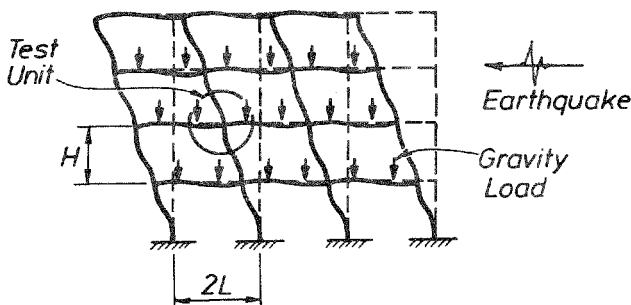


Fig. 1 Deflection Response of a Moment Resisting Frame to Lateral and Gravity Loading

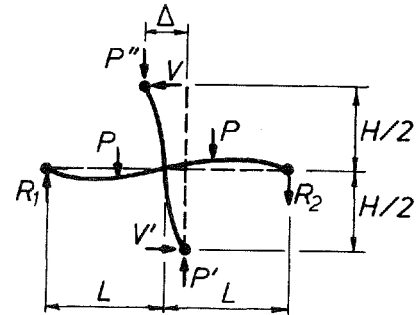


Fig. 2 The Isolated Subassemblage of the Frame with Loading

Units 1, 2, 3 and 4, are shown in Fig. 3. These beam-column units may be considered to be approximately three-quarters scale models.

2.2 Properties of Materials

2.2.1 Concrete

The ready mix concrete had a graded aggregate with a maximum size of 13 mm. Six 200 mm high by 100 mm diameter test cylinders, which had been cured in a fog room, were tested at the beginning of testing each Unit. The slump and average compressive strengths are shown in Table 1.

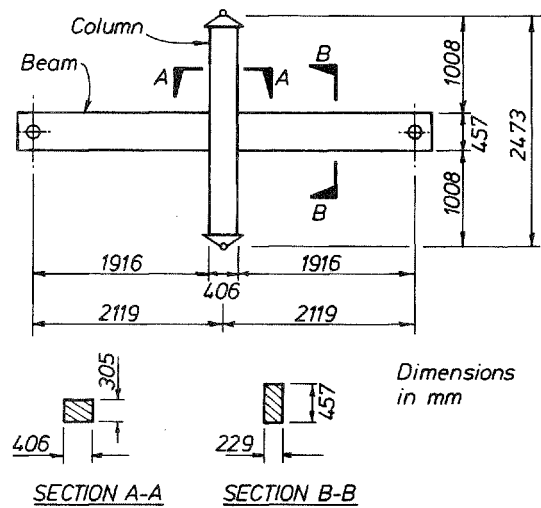


Fig. 3 Dimensions of Beam-Column Test Units 1, 2, 3 and 4

Table 1 Measured Concrete Properties

| Unit | 1 | 2 | 3 | 4 |
|------------------------------|------|------|------|------|
| Slump (mm) | 50 | 110 | 90 | 60 |
| Age at test of Unit (days) | 112 | 96 | 113 | 87 |
| f'_c at test of Unit (MPa) | 45.9 | 36.0 | 36.2 | 40.1 |

2.2.2 Reinforcing Steel

The average stress-strain curves measured for the reinforcing steel are plotted in Figs. 4, 5 and 6, and the measured properties are shown in Table 2. The deformed bars used for longitudinal reinforcement had a well defined yield point, but the plain round bars used for transverse reinforcement did not and the yield strength in that case was taken as the stress at a strain of 0.005 (see Fig. 4).

2.3 Design of Reinforcement

The details of the reinforcement for the four Units are shown in Figs. 7, 8, 9 and 10.

The longitudinal reinforcement in the beams was of Grade 275 deformed steel bar. The longitudinal top steel ratio ρ was 1.09% for Units 1 and 3 and 1.31% for Units 2 and 4. The longitudinal bottom steel ratio ρ' was 0.44% for Units 1 and 3 and 0.66% for Units 2 and 4. The longitudinal steel in the columns was of Grade 380 deformed steel bar and the longitudinal column steel ratio ρ_t was 1.30% for Units 1 and 2 and 1.16% for Units 3 and 4. The columns were designed to have an ideal flexural strength of at least 1.81 times the ideal flexural strength of the beams, as would be required by NZS 3101 (2) for ductile frames where columns are to be protected from plastic hinging.

The transverse reinforcement required for shear, for confinement of the concrete, and for the prevention of premature buckling of the longitudinal reinforcement in the beams and columns, was designed according to the requirements for ductile detailing of NZS 3101. The transverse reinforcement in the potential plastic hinge regions of the beams was governed by shear and was designed to resist the design shear forces assuming that no shear was carried by the concrete mechanisms ($V_c = 0$). In the columns it was governed by ϵ_c confinement.

The bond and shear requirements of the beam-column joint cores did not always satisfy the requirements of NZS 3101 for ductile detailing, as discussed below.

2.4 Design Variables Investigated in the Tests

The main design variables investigated were the development of the beam bars through the columns and the quantity of joint core shear reinforcement.

NZS 3101 gives specific design rules for the restriction of the diameter of the longitudinal bars in beams passing through the interior columns of ductile frames, but no rules are specified for the bar diameters in frames of limited ductility. One objective of this study was to investigate the current restriction on beam bar diameter for ductile frames and whether

Table 2 Measured Reinforcing Steel Properties

| Size | f_{yh} or f_y (MPa) | ϵ_y | E_s (MPa) | ϵ_{sh} | E_{sh} (MPa) | f_{su} (MPa) | ϵ_{sf} |
|--|----------------------------|--------------|----------------|-----------------|-------------------|-------------------|-----------------|
| (a) Used for Transverse Steel, Grade 275 Plain Round Bar | | | | | | | |
| R6(A) | 282 | 0.005 | 205,800 | | | 403 | 0.263 |
| R6(B) | 366 | 0.005 | 203,400 | | | 466 | 0.258 |
| R6(C) | 360 | 0.005 | 202,400 | | | 445 | 0.242 |
| R7 | 364 | 0.005 | 201,100 | | | 521 | 0.236 |
| R8 | 360 | 0.005 | 189,300 | | | 492 | 0.214 |
| R10 | 320 | 0.005 | 192,600 | | | 457 | 0.171 |
| R12 | 283 | 0.005 | 202,700 | | | 420 | 0.227 |
| (b) Used for Beam Longitudinal Steel, Grade 275 Deformed Bar | | | | | | | |
| D16 | 294 | 0.00140 | 210,400 | 0.0255 | 3,580 | 434 | 0.288 |
| D20 | 300 | 0.00143 | 210,300 | 0.0238 | 3,522 | 447 | 0.352 |
| D28 | 314 | 0.00156 | 200,700 | 0.0193 | 4,260 | 482 | 0.293 |
| (c) Used for Column Longitudinal Steel, Grade 380 Deformed Bar | | | | | | | |
| HD12 | 530 | 0.00263 | 201,900 | | | 698 | 0.202 |
| HD16 | 498 | 0.00253 | 196,600 | | | 660 | 0.198 |
| HD20 | 476 | 0.00242 | 197,100 | | | 644 | 0.198 |

Note: Key R6 = Plain round Grade 275 steel bar of 6 mm diameter
 D16 = Deformed Grade 275 steel bar of 16 mm diameter
 HD12 = Deformed Grade 380 steel bar of 12 mm diameter

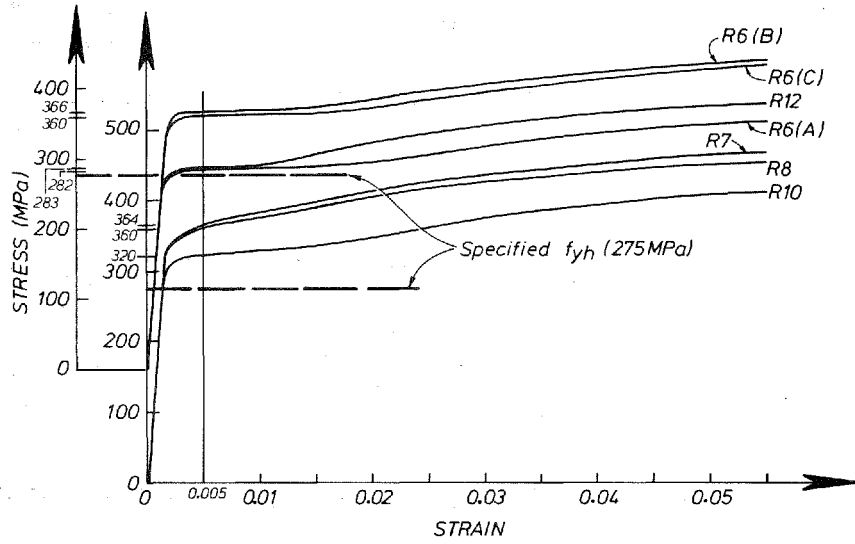


Fig. 4 Stress-Strain Curves for Transverse Reinforcing Steel

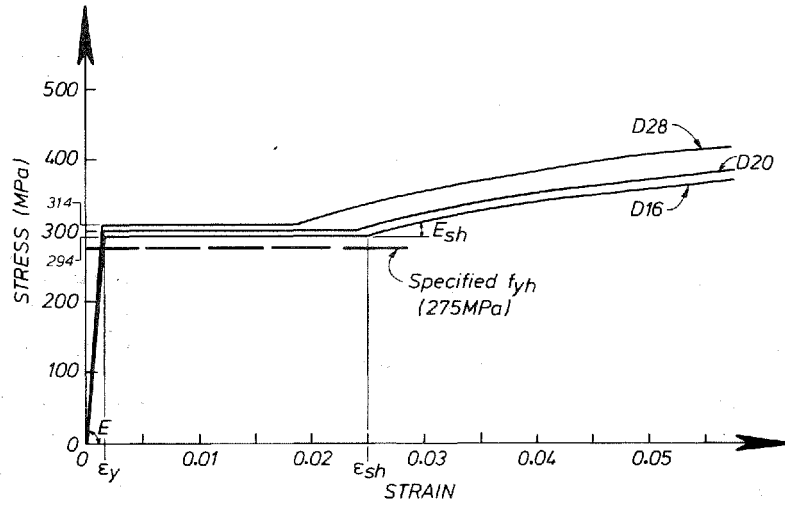


Fig. 5 Stress-Strain Curves for Beam Longitudinal Reinforcing Steel

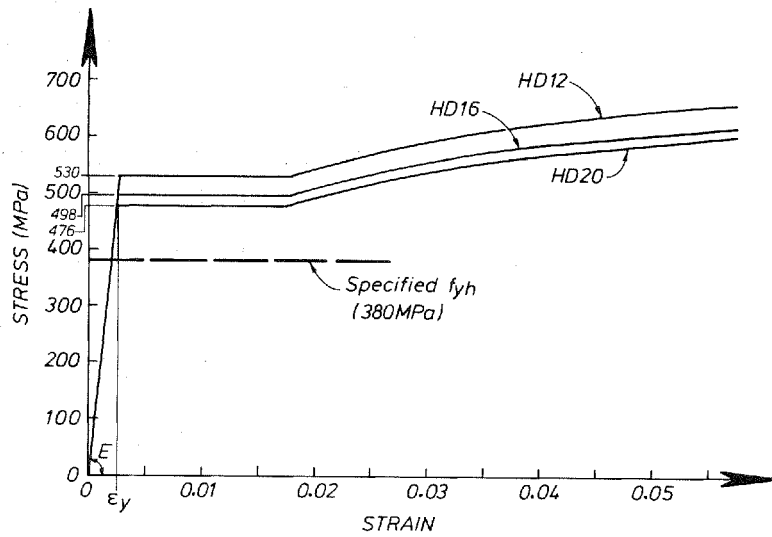


Fig. 6 Stress-Strain Curves for Column Longitudinal Reinforcing Steel

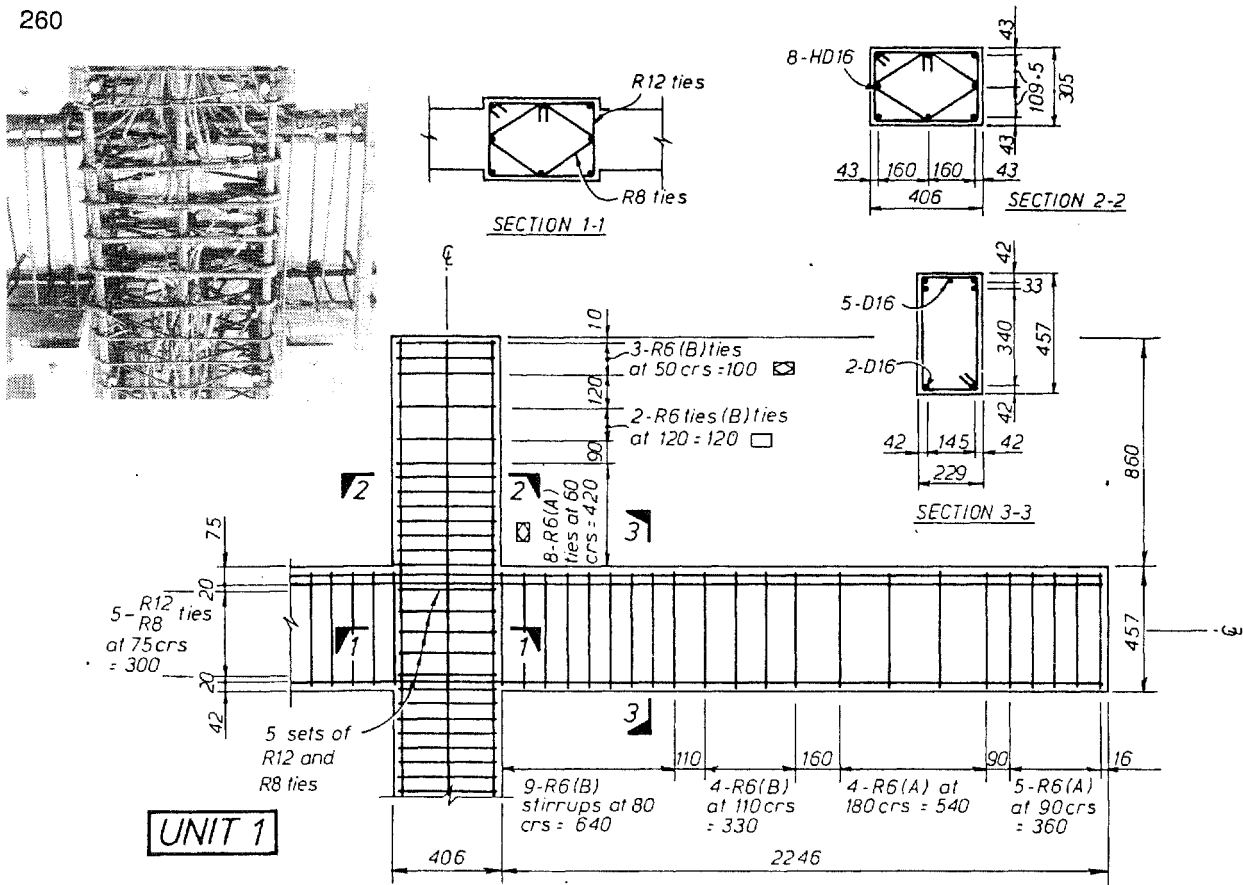


Fig. 7 Details of Reinforcement of Unit 1

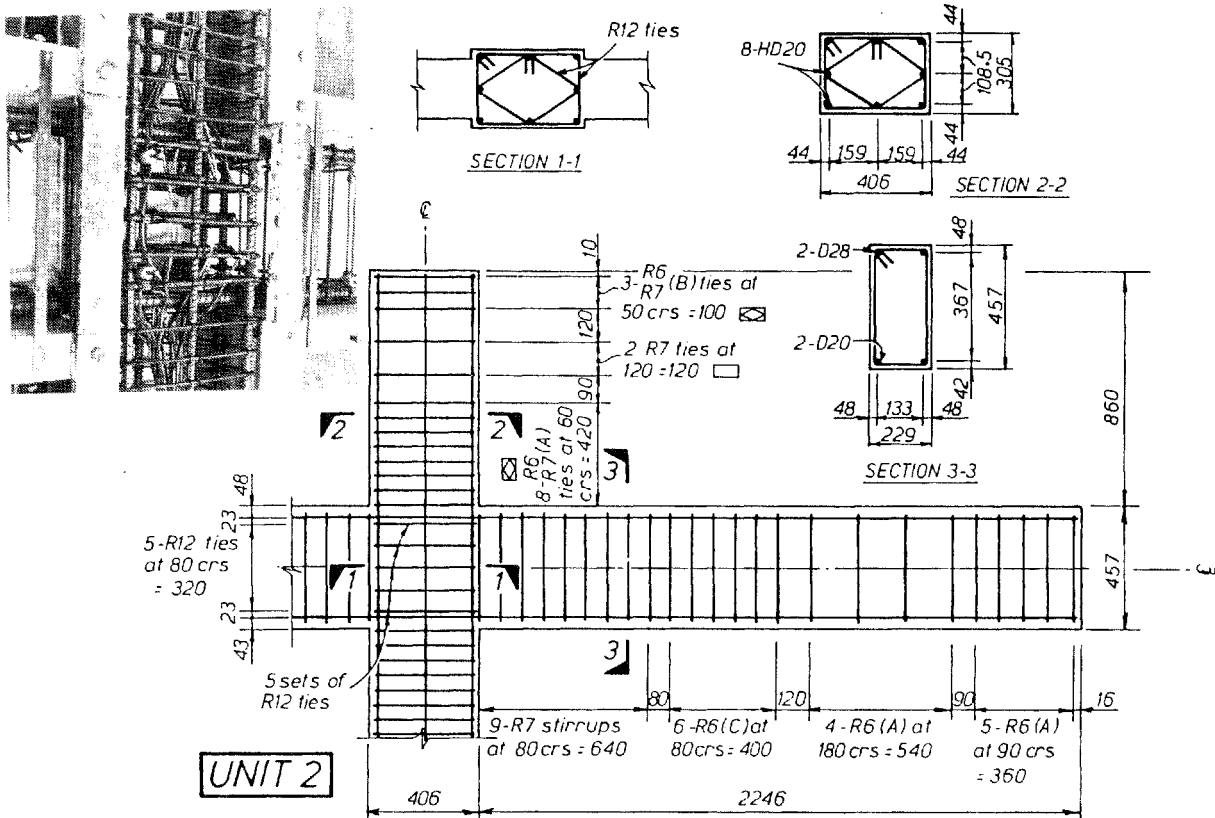


Fig. 8 Details of Reinforcement of Unit 2

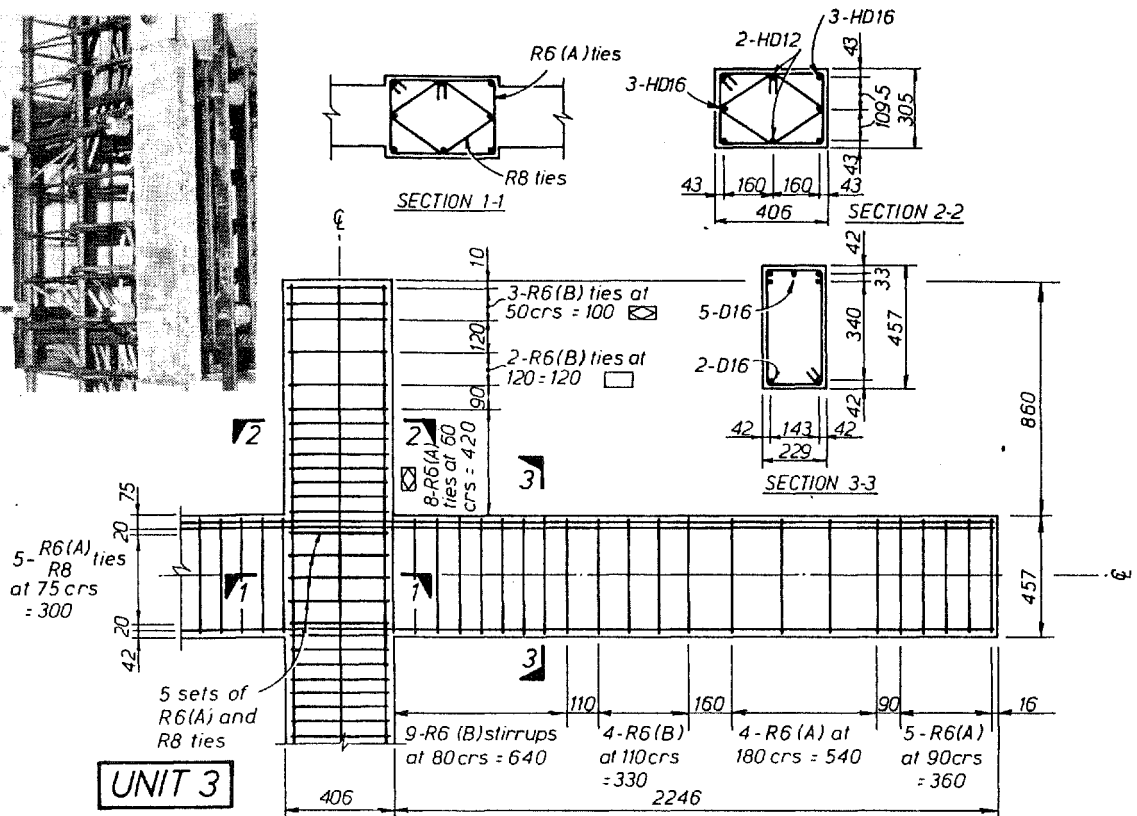
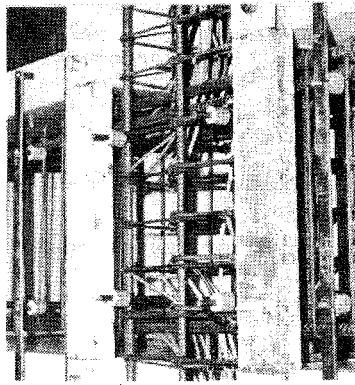


Fig. 9 Details of Reinforcement of Unit 3

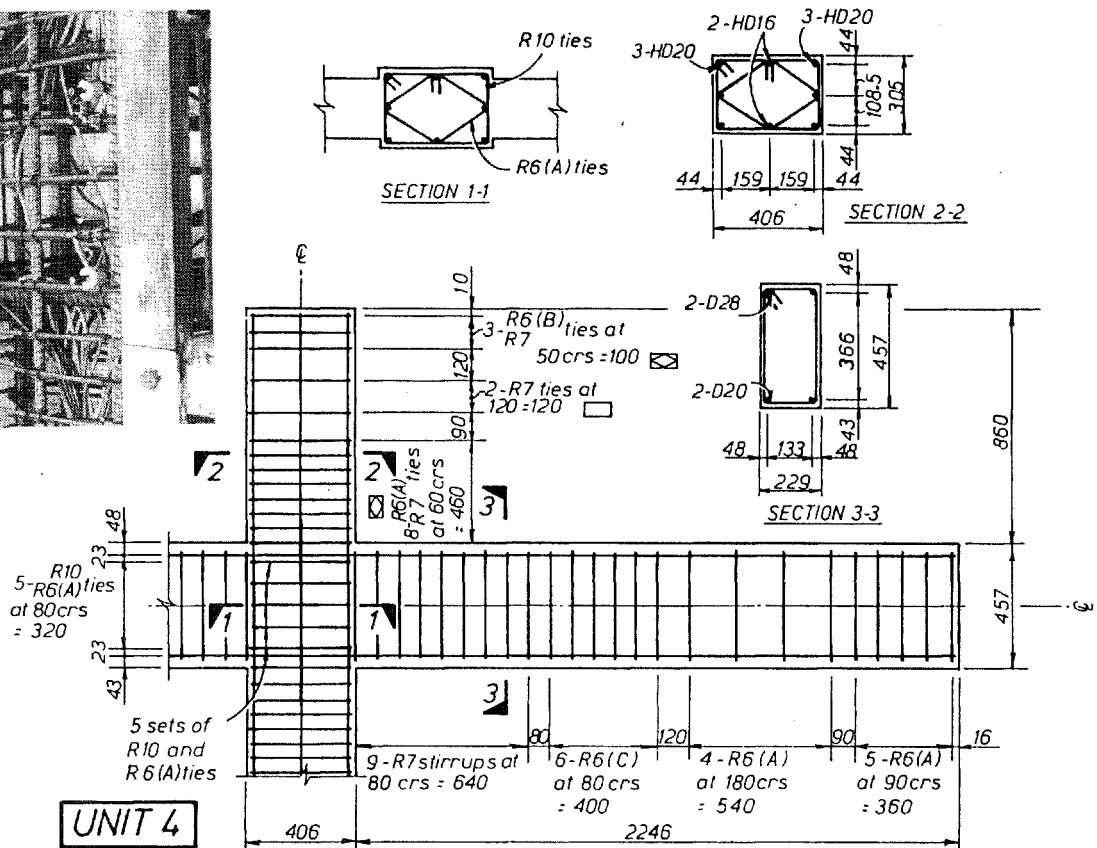
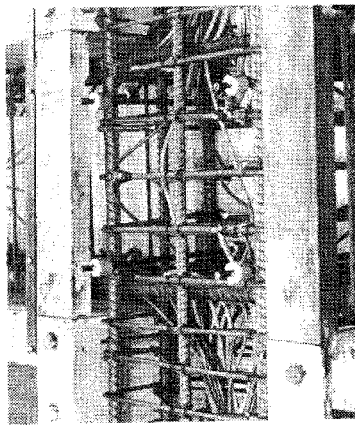


Fig. 10 Details of Reinforcement of Unit 4

any restriction is necessary for frames of limited ductility. For this reason in Units 1 and 3 the ratio of beam bar diameter to column depth satisfied the requirements of NZS 3101 for ductile frames, whereas in Units 2 and 4 larger beam bar diameters were used.

Also, NZS 3101 requires that for ductile frames with low axial load ($P_e/f'A_g \leq 0.1$, where P_e = design axial load on column, f'_c = concrete compressive cylinder strength and A_g = gross area of column) all the horizontal shear in the joint core should be transferred by shear reinforcement. That is, $V_{ch} = 0$ to account for the degradation in the shear transferred by the concrete diagonal compression strut during reversals of seismic loading. It is likely that for frames of limited ductility significant shear in the joint core could be considered to be carried by the concrete diagonal compression strut mechanism (that is $V_{ch} > 0$), even for low axial loads on columns. Another object of this study was to investigate the shear in the joint core resisted by the concrete diagonal compression strut mechanism in ductile frames and frames of limited ductility. For this reason in Units 1 and 2 the quantities of transverse hoops and intermediate longitudinal column bars placed in the joint core were the full amount required by NZS 3101 for ductile frames, while for Unit 3 and 4 the quantities were less than required for ductile frames. Table 3 compares the joint core shear forces required for ductile frames and with that provided by the shear reinforcement placed in the units. The design horizontal shear forces V_{jh} were calculated assuming that the stresses in the longitudinal beam reinforcement in the plastic hinge regions reach 1.15 times the actual measured yield strength of that steel due to strain hardening. This assumption is based on the previous finding that strain hardening of Grade 275 steel reinforcement causes the moment capacity of beams in plastic hinge regions to rise about 15% above that calculated using the measured yield strength (9). For these Units the measured yield strengths of the longitudinal beam steel were 1.07 to 1.14 times the specified yield strength. The design vertical shear forces were found

from $V_{jv} = V_{jh}h_b/h_c'$, where h_b = beam overall depth and h_c' = column overall depth. The joint core shear resistance provided by the reinforcement was calculated using the measured yield strengths of the transverse and vertical reinforcing steel.

2.5 Summary of Main Features of the Designs

The main features of the designs were as follows:

Unit 1 : The requirements for ductile detailing of NZS 3101 were followed in all respects.

Unit 2 : The requirements for ductile detailing of NZS 3101 were followed except that the diameter of the longitudinal beam bars was 72% greater than that permitted for the development of beam flexural reinforcement through columns. The ratio of the diameter of longitudinal beam bar to column depth was $d_b/h_c = 28/406 = 1/14.5$ whereas $1/25$ is the maximum value permitted for this ratio for Grade 275 deformed bars by NZS 3101 for ductile frames.

Unit 3 : The requirements for ductile detailing of NZS 3101 were followed except that in the joint core the horizontal shear reinforcement provided by hoops was 58% of that required, and the vertical shear reinforcement provided by intermediate column bars was 68% of that required.

Unit 4 : The requirements for ductile detailing of NZS 3101 were followed except that as for Unit 2 the diameter of the longitudinal beam reinforcement was 72% greater than that permitted, and as for Unit 3 in the joint core the horizontal shear reinforcement provided by the hoops was 58% of that required and the vertical shear reinforcement provided by intermediate column bars was 82% of that required.

Table 3 Comparison of Required Joint Core Shear Forces for the Units as Ductile Frames With Shear Forces Provided by Reinforcement

| Unit | 1 | 2 | 3 | 4 |
|-------------------------------------|------|------|------|------|
| Required $V_{sh} = V_{jh}$ (kN) | 390 | 544 | 392 | 545 |
| Provided V_{sh} (kN) | 470 | 585 | 229 | 317 |
| Provided/Required | 1.21 | 1.08 | 0.58 | 0.58 |
| Required $V_{sv} = 0.4 V_{jv}$ (kN) | 176 | 245 | 176 | 245 |
| Provided V_{sv} (kN) | 200 | 299 | 120 | 200 |
| Provided/Required | 1.14 | 1.22 | 0.68 | 0.82 |

Note: The nominal horizontal joint core shear stress was less than $1.5 \sqrt{f'_c}$ MPa

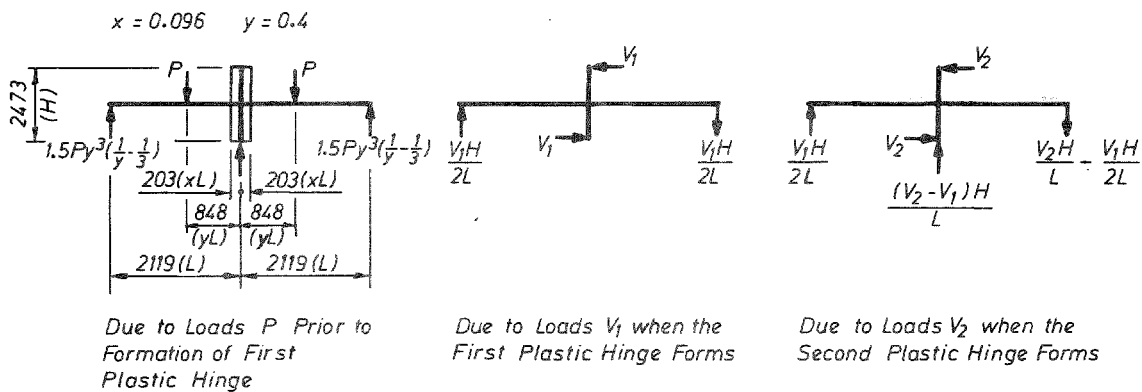
2.6 Details of Loading

The Units were loaded under both simulated seismic and gravity loading. In these tests a single point load applied to each span was used to simulate gravity loading.

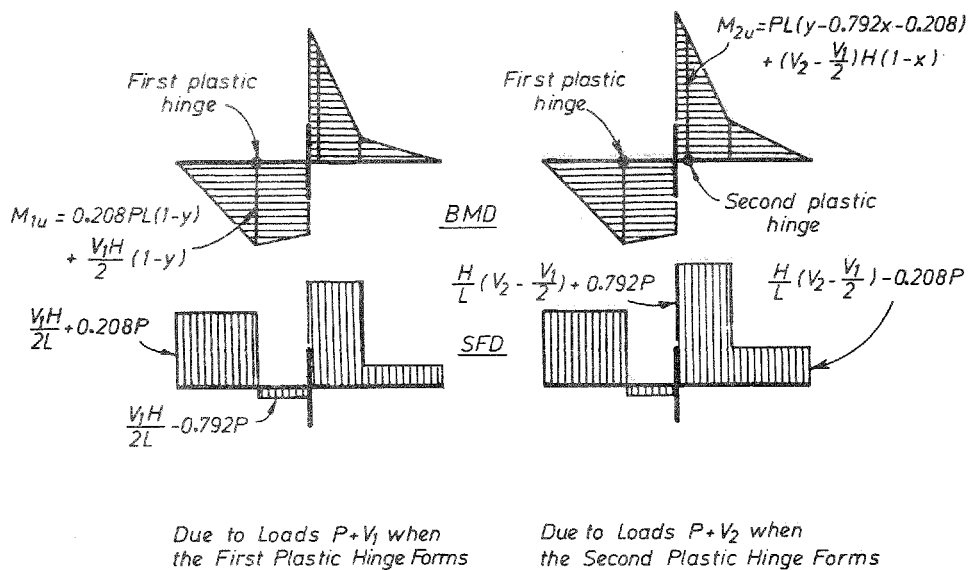
Figure 11 shows the loading of the Units and the bending moment and shear force diagrams for the beams at the stages when the first and second plastic hinges formed. It was considered desirable in the tests for the positive bending moments in the region between the point of gravity load and the column face to be nearly horizontal, in order to obtain the critical situation for the joint core in which the beam steel is yielding or near yielding at both column faces. In this study $y = 0.4$

was assumed, in which yL is the distance from the gravity load point to the column centre where L is the length of the beam from the end reaction point to the column centre (see Fig. 11a).

When loading a Unit, first the two gravity loads P were applied to the beams. Next, the horizontal load was applied to the column tops and increased from zero to V_1 , at which stage the first plastic hinge appeared in the left hand beam close to the point of application of the gravity load. Then, the horizontal load applied to the column tops was increased to V_2 , at which stage the second plastic hinge formed in the right hand beam adjacent to the column face. It is evident that significant redistribution of the bending moments and shear was required to occur in the right



(a) Actions



(b) Bending moment and shear force diagrams when plastic hinges form in beams.

Fig. 11 Bending Moment and Shear Force Diagrams for the Beams at Various Stages of Loading

hand beam when the horizontal load was increased from V_1 to V_2 .

The horizontal loads V_1 and V_2 , when the first and second plastic hinges form, can be shown to be

$$V_1 = \frac{1}{0.3 H} (M_{1u} - 0.125 PL) \quad (1)$$

$$V_2 = \frac{1}{0.904 H} (M_{2u} - 0.116 PL) + \frac{V_1}{2} \quad (2)$$

In this study $P = 55 \text{ kN}$ was chosen for Units 1 and 3 and $P = 67 \text{ kN}$ was chosen for Units 2 and 4. The values for the theoretical flexural strengths of the beams for positive and negative moments, M_{1u} and M_{2u} respectively, calculated using the approach of NZS 3101 (2) from the beam dimensions and reinforcing steel areas, are listed in Table 4. These theoretical flexural strengths were calculated using the actual material strengths but ignoring strain hardening of steel, and assuming an extreme fibre concrete compressive strain of 0.003, a rectangular concrete compressive stress block with a mean stress of $0.85 f'_c$ and a strength reduction factor $\phi = 1$.

The resulting V_1 and V_2 values given by Eqs. 1 and 2 for those values for P , M_{1u} , M_{2u} and for $H = 2.473 \text{ m}$ and $L = 2.119 \text{ m}$ are also listed in Table 4. Note that the ratio of P/V_1 used in the tests was 1.045 for Units 1 and 3 and 0.846 for Units 2 and 4.

In the tests no compressive axial load was applied to the upper end of the column. Hence the joint core was tested under a disadvantageous loading condition.

Table 4 Theoretical Flexural Strengths of Beams for Positive and Negative Moments M_{1u} and M_{2u} , Load P , and Horizontal Loads at Column Tops When the First and Second Plastic Hinges Form V_1 and V_2

| Units | | 1 | 2 | 3 | 4 |
|----------|-----|-------|-------|-------|-------|
| M_{1u} | kNm | 54.8 | 78.9 | 51.6 | 76.9 |
| M_{2u} | kNm | 114.8 | 146.4 | 115.4 | 148.0 |
| P_{2u} | kN | 55.0 | 67.0 | 55.0 | 67.0 |
| V_1 | kN | 54.2 | 78.9 | 50.0 | 79.7 |
| V_2 | kN | 72.6 | 97.8 | 70.8 | 98.9 |

3. TEST PROGRAMME

3.1 The Test Rig

The test rig used is shown in Figs. 12 and 13. The in-plane horizontal load was applied to the column top by a double acting 300 kN capacity MTS hydraulic jack. A strain gauged load cell was placed between the jack and a link bar connected to the top hinge. The jack could be load or displacement controlled.

Two in-plane vertical loads, which simulated the gravity loads, were applied to the beam at points 848 mm from the centre line of column and held constant during the tests. These loads were applied by 100 kN capacity jacks acting through load cells and steel rods connected to steel pivot blocks placed on the surface of the beam. The pivot blocks allowed free rotation there and horizontal movement of the beam in-plane.

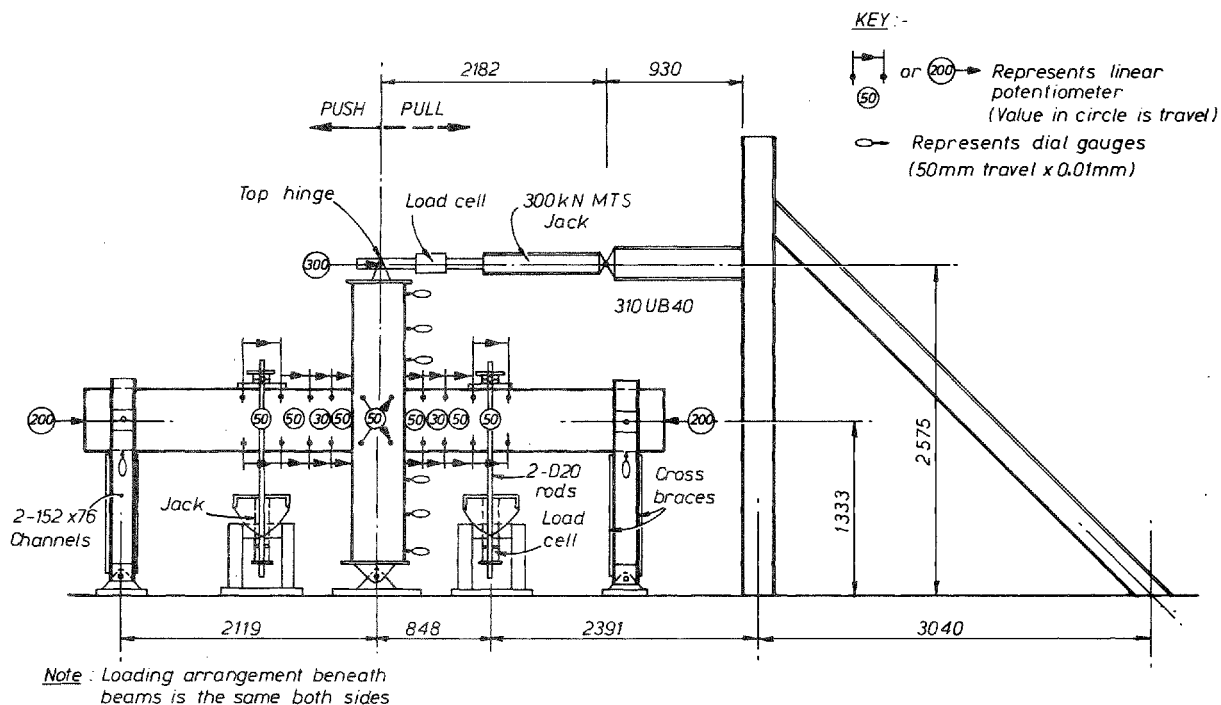


Fig. 12 The Test Rig

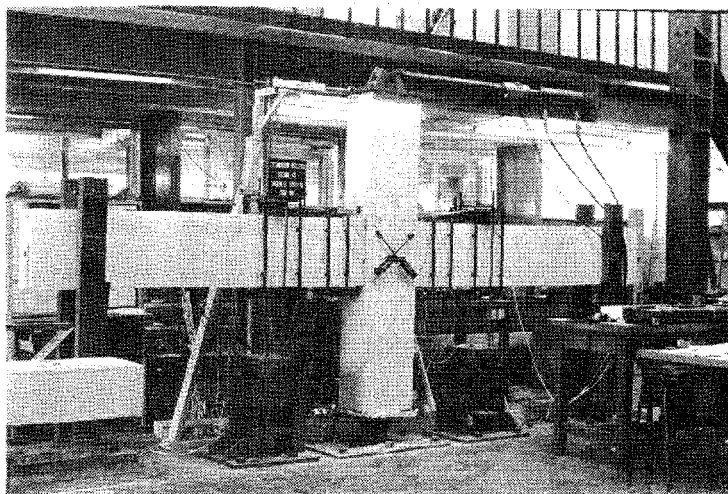
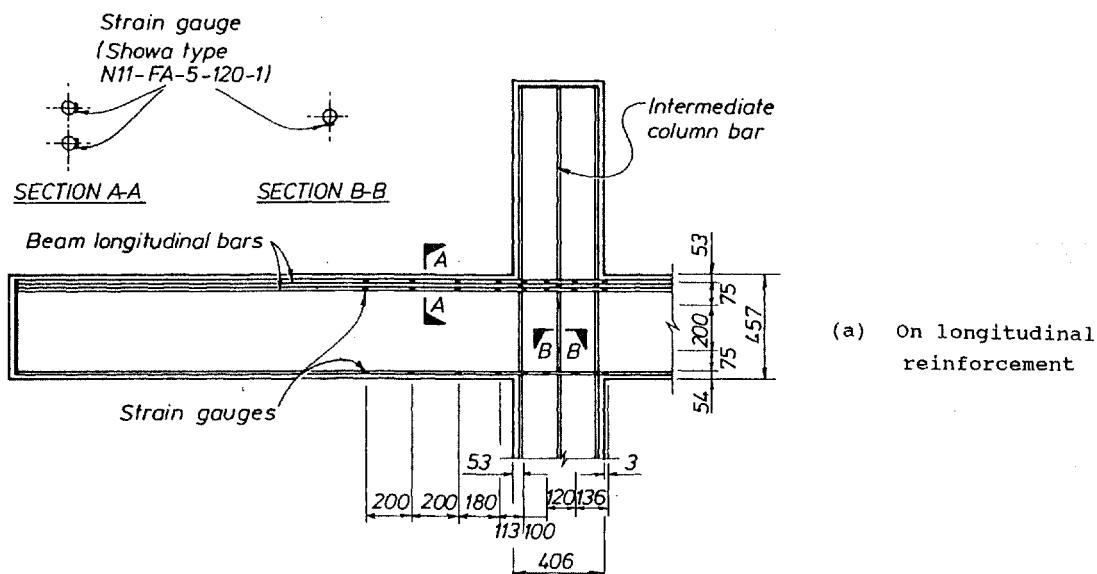


Fig. 13 An Overall View Showing a Test in Progress



Each end of the beam was held against vertical displacement using two 152 x 76 steel channels, one on each side of the beam, and a 40 mm diameter steel pin which provided the vertical reactive forces to the beam. This connection allowed free horizontal movement and rotation of the beam but not vertical displacement.

To measure the column deflections and beam curvatures in the regions near the column faces a number of Sakai linear potentiometer were used as shown in Figs. 12 and 13.

Electrical strain gauges, consisting of Showa Type N11-FA-5-120-1, were placed on some longitudinal reinforcing bars in the beams and columns and on joint core hoops, as shown in Fig. 14. The strain gauges on the longitudinal beam and column bars were attached to the mid-depth of the bar so as to eliminate as far as possible strains due to bending of the bar. The strain gauges on the joint core hoops were attached in pairs above and below the hoop

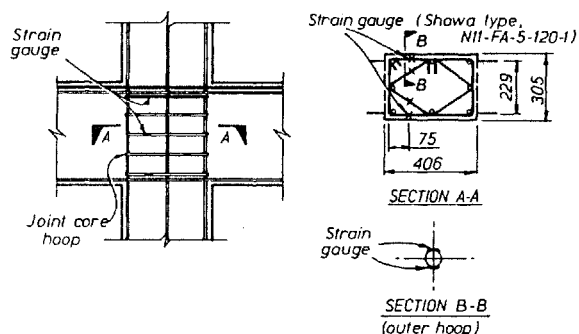


Fig. 14 Position of Electrical Resistance Strain Gauges on Reinforcing Steel of Units

bar in the direction of shear transfer and the average value of strain for the pair was taken, thus eliminating the effect of bending strains due to bowing out of the hoops.

The shear distortion of the joint core was measured using pairs of 50 mm travel linear potentiometers placed diagonally on each side face of the joint (see Figs. 12 and 13). The average values measured from each pair of linear potentiometers were used.

3.2 Loading Sequence

The cyclic loading pattern used in the tests involved imposed displacement ductility factors μ following the pattern shown in Fig. 15. The displacement ductility factors were increased gradually in order to observe performance in the "limited ductility" range as well as in the "ductile" range.

In the first cycle of lateral loading, the beam-column unit was taken to three-quarters of the theoretical horizontal ultimate load in both directions, calculated on the basis of the actual measured material strengths, and the corresponding deflections of column top in the two directions, Δ_{y1} and Δ_{y2} , were measured. The first yield displacement for the Unit was then taken as

$$\Delta_y = \frac{4}{3} \left[\frac{1}{2} (\Delta_{y1} + \Delta_{y2}) \right] \quad (3)$$

and the displacement ductility factor was defined as

$$\mu = \Delta / \Delta_y \quad (4)$$

The theoretical horizontal ultimate load was taken as V_2 which is the load at which both the first and the second plastic hinges had formed (see Fig. 11), given by Eq. 2 and listed for the units in Table 4.

Before the testing commenced the vertical reaction forces at both ends of the beam were checked and it was confirmed that those forces were close to zero. Then the vertical loads were applied and were not changed during the test. When the lateral load was applied to the column top the vertical movements at both ends of the beam were monitored and found to be insignificant. Possible out-of-plane instability of the unit was prevented by a pair of cross braces at each end of the beam.

4. TEST RESULTS AND OBSERVATIONS

4.1 General Results and Observations

The experimentally obtained hysteresis loops, which plot horizontal load at the column top versus horizontal displacement there, are shown in Fig. 16a, b, c and d. Also shown in those figures are the theoretical horizontal loads when the first plastic hinge formed at the critical positive moment section V_1 and the theoretical horizontal load when the second plastic hinge formed at the critical negative moment section V_2 . The horizontal displacements are also shown as displacement ductility factors and drifts (horizontal displacement of storey/storey height).

The positive moment plastic hinge in the beam of each unit tended to form in the region adjacent to the the column face. The positive bending moment in the region between the column face and the gravity load point was almost constant, and the

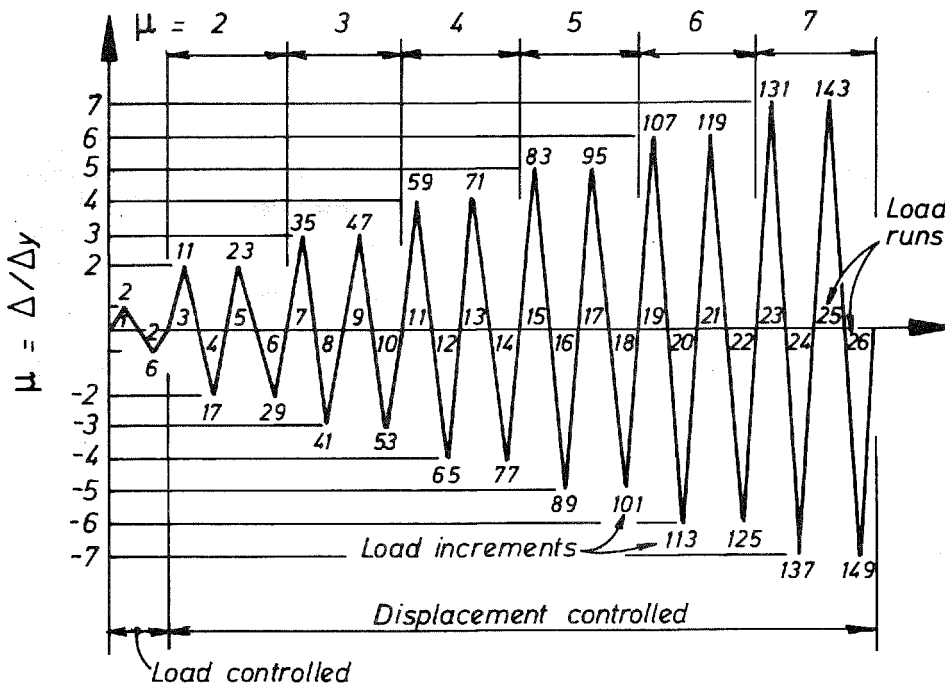
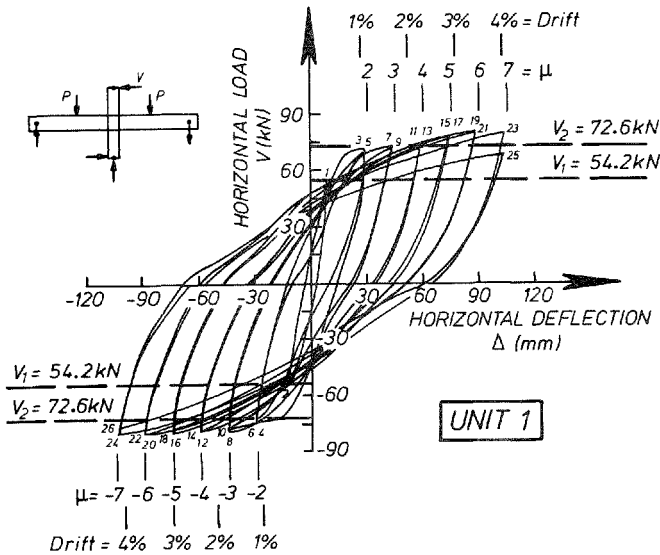
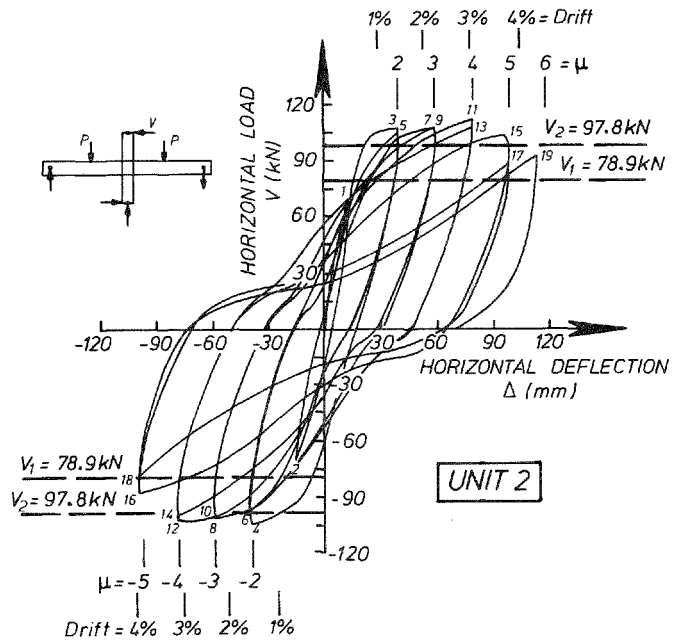


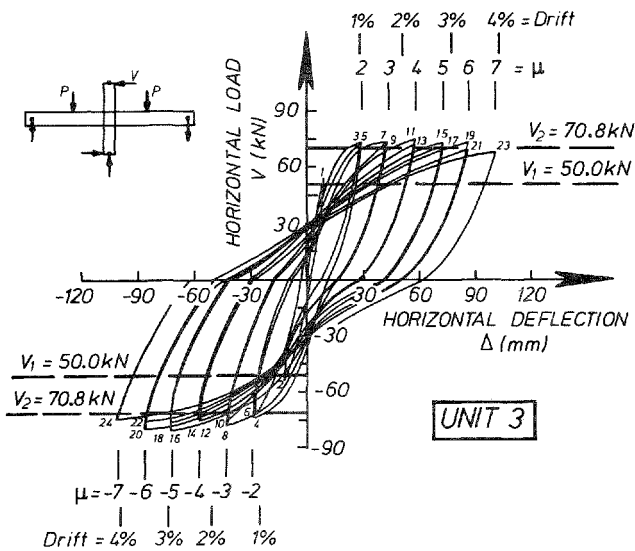
Fig. 15 Cyclic Load Sequence Used in the Tests



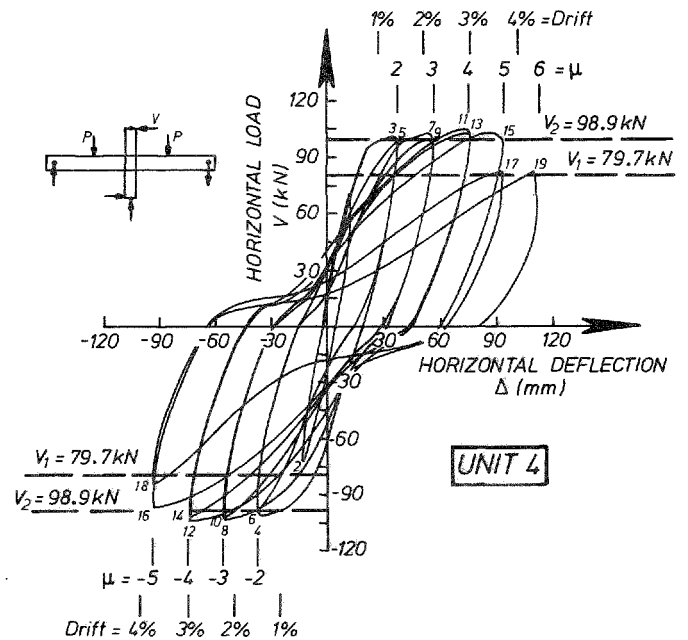
(a) Unit 1



(b) Unit 2



(c) Unit 3



(d) Unit 4

Fig. 16 Measured Horizontal Load Versus Horizontal Displacement Hysteresis Loops

associated cracking was vertical. The negative moment plastic hinge formed in the beam in the region adjacent to the column face and the associated cracking was inclined due to the influence of shear (see Fig. 13). Limited cracking only appeared in the columns during testing, since the columns remained in the elastic range. More extensive cracking occurred in the joint core regions of the columns, in the form of inclined diagonal tension cracking.

It is evident from Fig. 16a that the behaviour of Unit 1, which had been designed according to the provisions for ductile frames of NZS 3101 (2), was excellent. The Unit maintained its strength, stiffness and energy dissipation characteristics well during the cyclic loading. The maximum surface crack widths measured at a displacement ductility factor $\mu = 2$ was 1.8 mm on the beam and 0.2 mm on the joint core. First spalling of the

compressed cover concrete of the beam was observed at $\mu = 3$. The maximum crack width measured on the joint core during testing was 0.6 mm. Cracking of the joint core was evidently well controlled by the joint core shear reinforcement.

From Fig. 16b it is evident that Unit 2 showed a greater reduction in stiffness than Unit 1 during the cyclic loading. The hysteresis loops became quite pinched at $\mu = 5$, no doubt due to bond degradation leading to some slip of the larger diameter beam bars through the column. First spalling of the compressed cover concrete of the beam was observed at $\mu = 3$. The maximum crack width measured on the joint core during testing was 0.4 mm and diagonal tension cracking there was again evidently well controlled by the joint core shear reinforcement.

From Fig. 16c it can be seen that Unit 3 showed a greater reduction in stiffness than Unit 1 during the cyclic loading. However the hysteresis loops were not as pinched as for Unit 2 at $\mu = 5$. First spalling of the compressed cover concrete of the beam was observed at $\mu = 3$. The maximum crack width measured on the joint core during testing was 1.4 mm, which was significantly larger than for Units 1 and 2, due to the smaller quantity of joint core horizontal shear reinforcement and the significant yielding of that steel.

From Fig. 16d it can be seen that Unit 4 also demonstrated a greater reduction in stiffness than Unit 1 during cyclic loading. The hysteresis loops were as pinched as for Unit 2. First spalling of the compressed cover concrete of the beam was observed at $\mu = 3$. The maximum crack width measured on the joint core during testing was 1.1 mm, again due to significant yielding of the joint core shear reinforcement.

The maximum experimental horizontal loads V_{max} reached by Units 1, 2, 3 and 4 during the tests were 80.3, 111.7, 79.4 and 106.5 kN, respectively. The ratios of V_{max}/V_2 for Units 1, 2, 3 and 4 were 1.11, 1.14, 1.12 and 1.08, respectively, where V_2 = theoretical ultimate horizontal load calculated for the Units. The strength degradation of Unit 1 at the end of testing was small. At the end of the last loading run of Units 2, 3 and 4 the horizontal load carried had reduced to 76%, 99% and 81% of the theoretical ultimate load V_2 , respectively.

4.2 Behaviour of the Beam-Column Joint Cores

The pairs of potentiometers placed diagonally on the side faces of the beam-column joint cores indicated that the contribution of the shear deformation of the joint cores to the total horizontal displacement at the column tops increased during cyclic loading. Eventually at high displacement ductility factors this contribution was 9 to 14% for Unit 1, 7 to 12% for Unit 2, 23 to 38% for Unit 3, and 15 to 19% for Unit 4. Hence for Units 1 and 2 which had joint core reinforcement as required by NZS 3101 (2) for ductile

detailing the joint core deformations were kept relatively small, but for Units 3 and 4 with lesser joint core reinforcement the joint core deformations were significantly larger. It is noticeable that Unit 4 with larger diameter beam bars had a smaller joint core deformation than Unit 3 which had smaller diameter beam bars. Both units had the same joint core shear reinforcement. Hence some slip of longitudinal steel through the joint evidently permitted the open flexural crack in the beam at the column face to tend to close even when the large area of top beam steel was in compression. As a result the joint core became less flexible because the joint core shear could then be transferred by relatively stiff diagonal compression strut rather than a more flexible truss mechanism. The greater stiffness of the joint core of Unit 2 compared with Unit 1, for the same reason, is also noticeable.

Figure 17 illustrates the joint core strains measured at various displacement ductility levels on the rectangular hoops of the Units. The strains measured on the diamond shaped hoops in the joint cores were similar to those on the rectangular hoops. The yield strain of the joint core reinforcement was 1.4×10^{-3} . The hoops in the joint core of Units 1, 3 and 4 reached yield and in Unit 2 the hoops almost reached yield. It is apparent that the hoop strains in the joint core of Units 1 and 2 did not increase beyond twice the yield strain, but in Units 3 and 4 higher hoop strains were reached. In the case of Unit 3 the hoop strains eventually approached four times the yield strain. Figure 18 compares the visible cracking of the joint cores of Units 1 and 3 at $\mu = 7$. Unit 3 has an extensive diagonal tension crack whereas for Unit 1 the diagonal tension cracks were of smaller width.

It was also noticeable that the joint core of Unit 4 after testing was not as badly cracked as for Unit 3. That is, when some slip of the larger diameter top beam bars of Unit 4 occurred, and the flexural crack in the beam at the column face tended to close, more shear was transferred by the concrete diagonal compression strut mechanism. Hence the joint core in Unit 4 was subjected to less shear deformation than in the case of Unit 3.

Figure 19 illustrates the variation in the strain along the intermediate longitudinal column bars measured at five points within the joint cores at various ductility levels for the Units. These column bars were at the mid-depth of the column section and, according to the truss mechanism for shear transfer in the joint core, are needed for vertical shear reinforcement. Figure 19 shows that these bars were in tension above and below the joint core, as would be expected from their role as flexural reinforcement in a column which is carrying small external axial load. The bars did not reach yield but the stress in the bars within the joint core was significantly higher than the stress in the bars at the top and bottom of the joint core, which is consistent with their additional role as vertical shear reinforcement in joint cores.

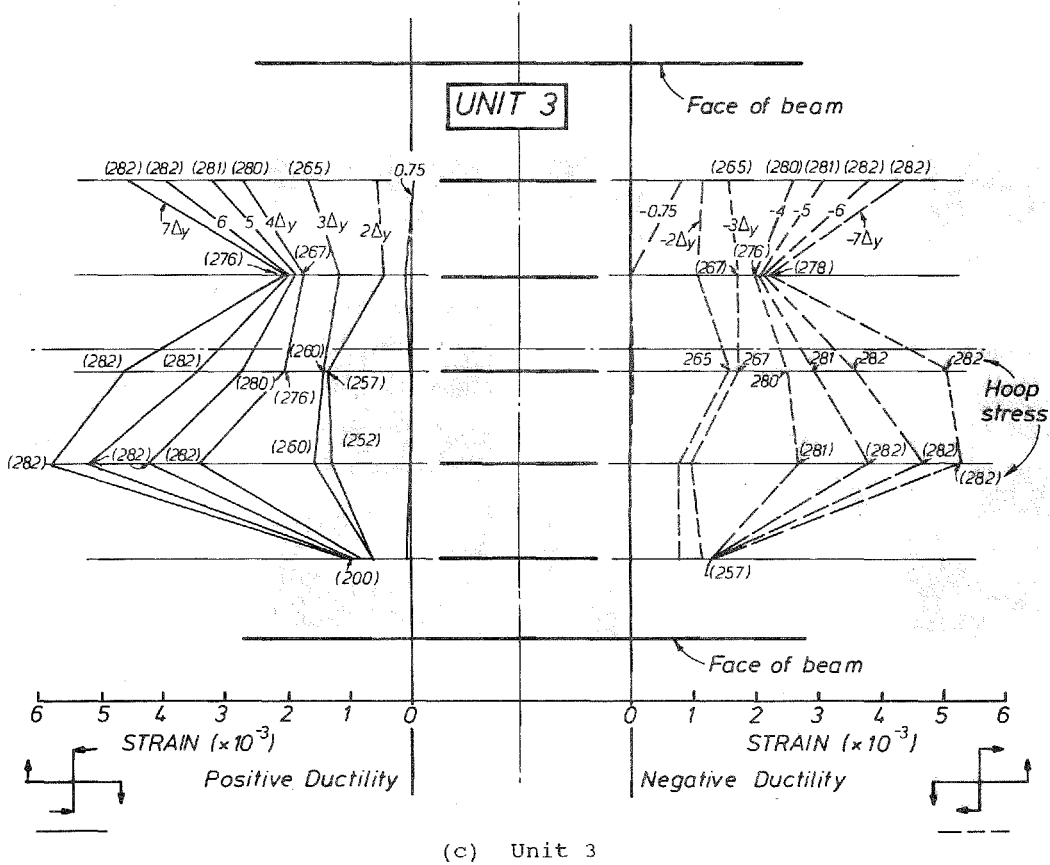
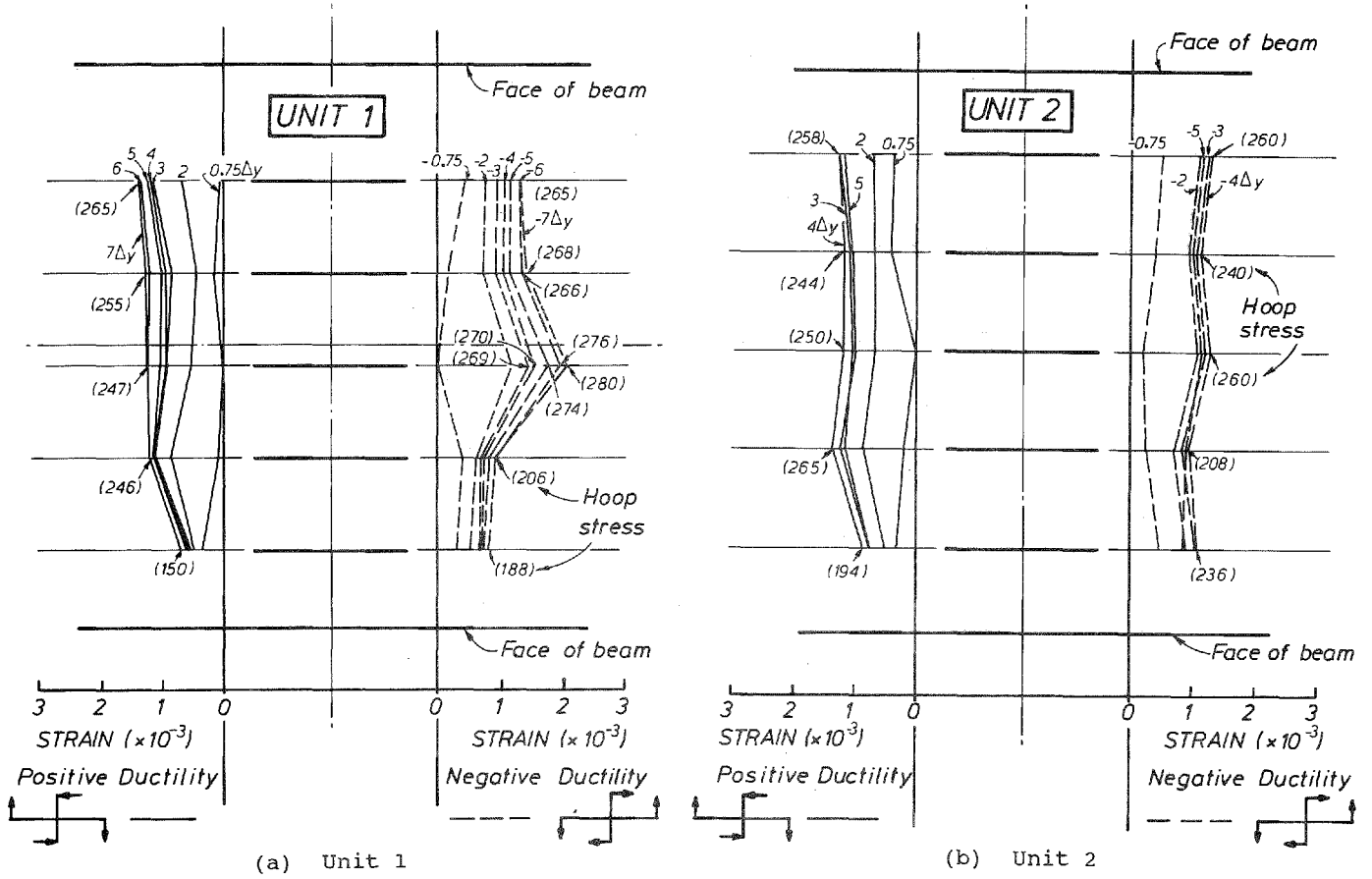


Fig. 17 Joint Core Strains Measured at Various Displacement Ductility Levels on the Rectangular Hoops (Continued on Next Page)

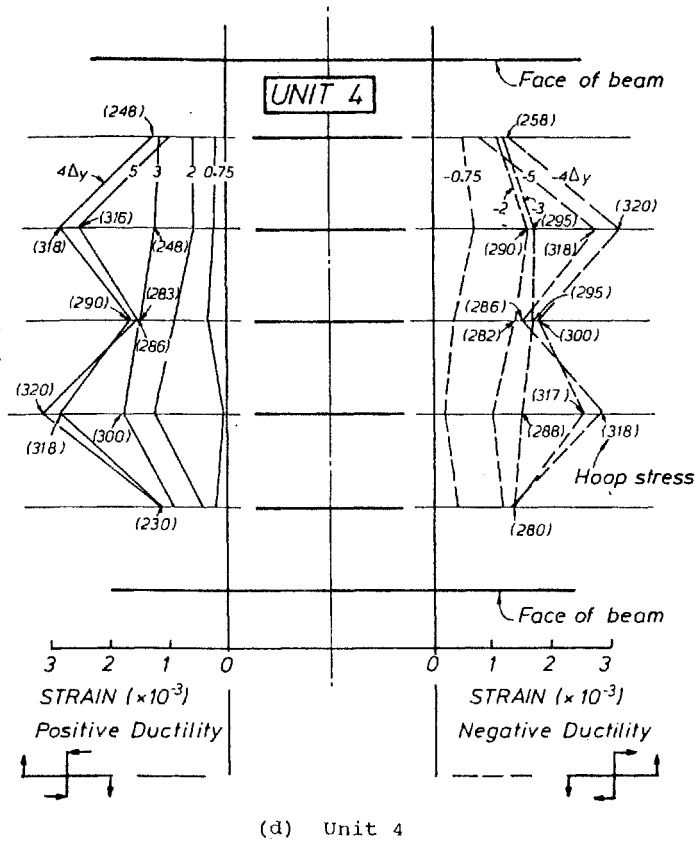
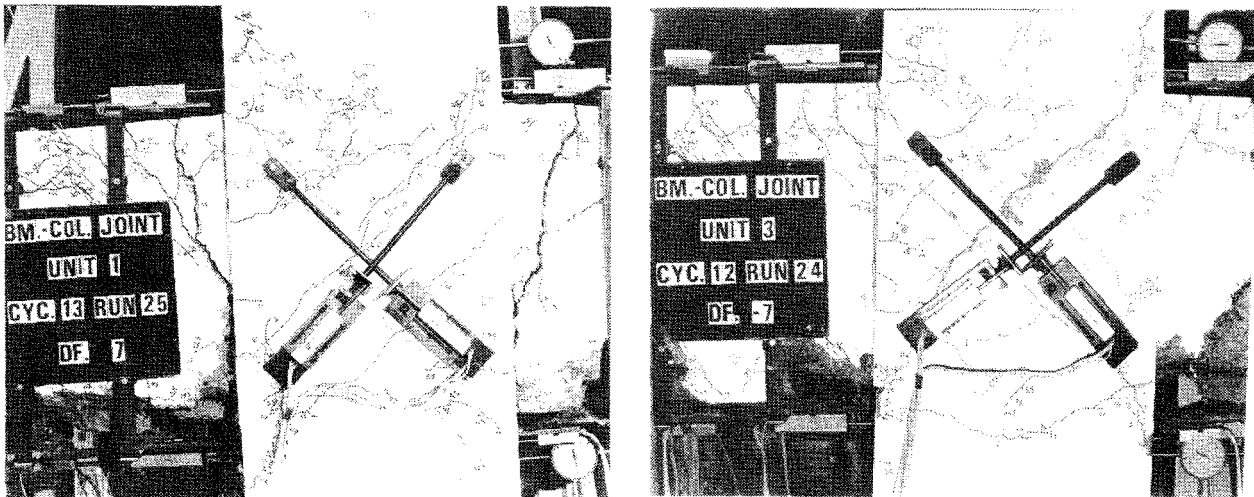


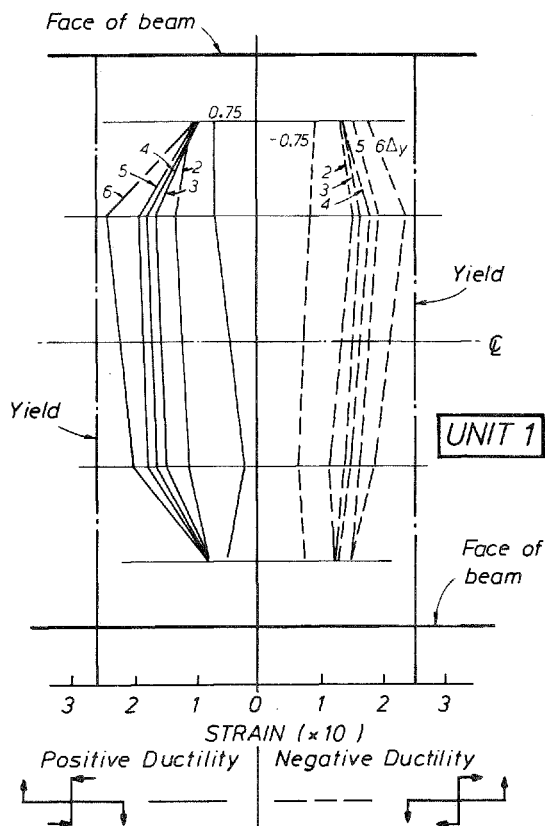
Fig. 17 Joint Core Strains Measured at Various Displacement Ductility Levels on the Rectangular Hoops (Continued from Previous Page)



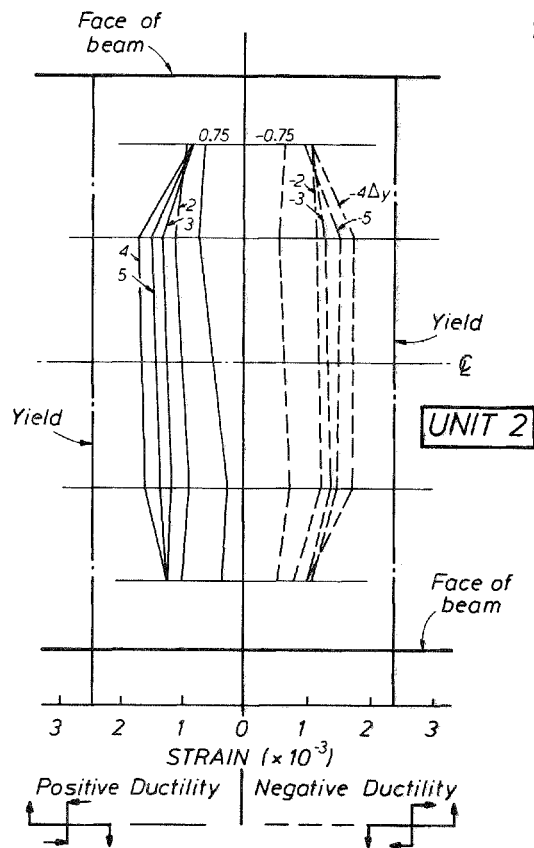
(a) Unit 1

(b) Unit 3

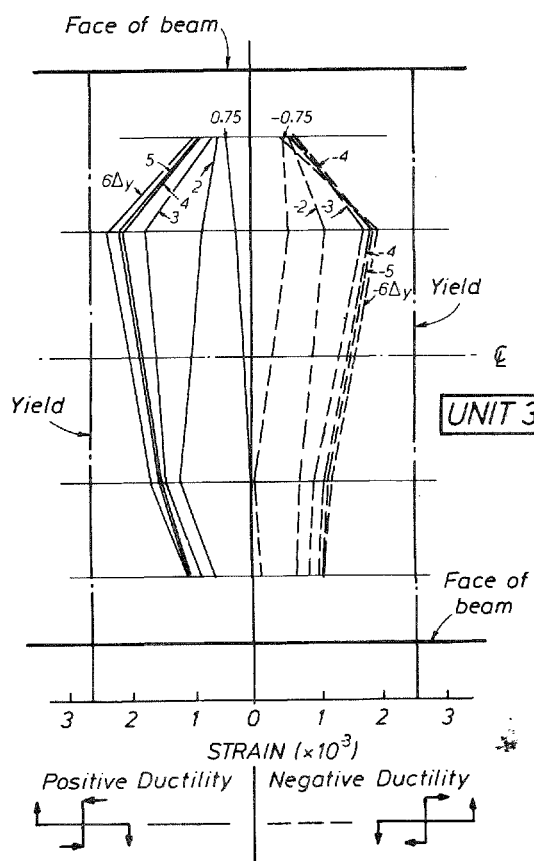
Fig. 18 Comparison of Cracking of the Joint Regions of Units 1 and 3 at Displacement Ductility Factor of 7



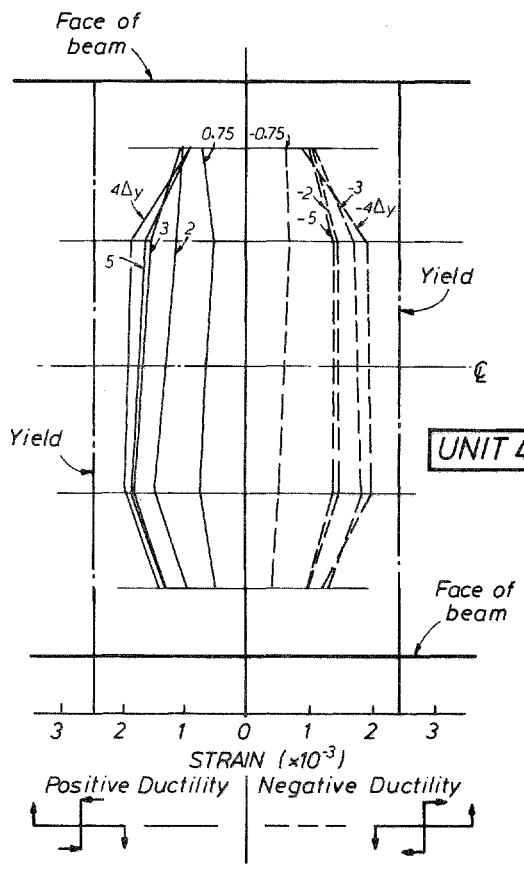
(a) Unit 1



(b) Unit 2



(c) Unit 3



(d) Unit 4

Fig. 19 Joint Core Strains Measured at Various Displacement Ductility Factor Levels on the Intermediate Longitudinal Column Bars

Figure 20 illustrates the variation of strain measured on the longitudinal top and bottom bars of the beams of Units 1 and 2 at four points within the joint and at three points to one side of the column in the beam plastic hinge region. The measurements on the top and bottom beam bars showed extensive yielding in tension which penetrated into the joint core. However the bar stresses were generally at less than yield in the middle one-quarter of the joint core, indicating that even with some slip of beam steel due to bond degradation there was significant transfer of bar force to the concrete of the joint core by bond. During the moment reversals the top beam bars yielded only in tension, as would be expected since the area of bottom steel in the beam was smaller and hence unable to yield the top steel in compression. The bottom beam bars yielded in both tension and compression in the beams, as would be expected, but yielded only in tension in the joint core.

5. DISCUSSION OF DESIGN ASSUMPTIONS FOR BEAM-INTERIOR COLUMN JOINT CORES

5.1 Joint Core Shear Design

The Units were loaded cyclically in the inelastic range with imposed displacement ductility factors of 2 cycles at each $\mu = \pm 2, \pm 3, \pm 4, \pm 5$ and some times higher. Hence all Units were subjected to a performance test at ductility levels required for "ductile" structures according to NZS 4203 (1). It is apparent that all Units satisfied the required performance criterion of undergoing cyclic lateral loading equivalent to four cycles to $\mu = \pm 4$ without the lateral load carrying capacity reducing by more than 20%.

Units 3 and 4 contained 58% of the horizontal joint core shear reinforcement, and 68% and 82% respectively of the vertical joint core shear reinforcement, required for ductile structures by NZS 3101. Plastic hinging occurred in the beams at the column faces of both Units, as may be observed from the strain distributions for the beam longitudinal bars shown in Fig. 20.

It appears from the test results for these Units that the NZS 3101 (2) design assumption which neglects the joint core shear carried by the concrete diagonal compression strut mechanism (that is, assuming $V_{ch} = 0$) when the axial load level is low ($P_e \leq 0.1 f'_c A_g$) is unduly conservative. Evidently, even when plastic hinging occurs in the beams at the column faces, some longitudinal beam reinforcement force can be transferred to the concrete diagonal compression strut mechanism by bond from the bars at the end region of the strut (see Fig. 21). Considerations in the past (6,7) have concluded that the penetration of yielding of the longitudinal beam reinforcement into the joint core concentrates the bond stresses near the centre of the joint, thus reducing significantly the contribution of the concrete diagonal compression strut mechanism to the transfer of horizontal joint core shear. However the test results

from these Units do indicate that this reduction in shear carried by that strut mechanism may not be so serious. Hence the horizontal joint shear force required to be transferred by the truss mechanism may be significantly less than the total horizontal shear force.

On the basis of these test results it can be concluded that for the case where unsymmetrical beam reinforcement was used (in Units 3 and 4 the ratio of bottom to top steel areas was 0.4 and 0.5 respectively), the concrete diagonal strut mechanism transferred at least 42% of the total horizontal joint core shear. Hence for beam-column joints with low axial load ($P_e \leq 0.1 f'_c A_g$, where P_e = axial load on the column, f'_c = concrete compressive cylinder strength and A_g = gross area of the column), it could be recommended that the horizontal joint core shear force to be resisted by the concrete mechanism of ductile structures be taken as

$$V_{ch} = 0.4 V_{jh} \quad (5)$$

and hence that sufficient horizontal shear reinforcement should be present to resist

$$V_{sh} = 0.6 V_{jh} \quad (6)$$

where V_{jh} = design horizontal joint core shear force.

It is likely that Eqs. 5 and 6 could also be used for beams with symmetrical reinforcement (equal areas of top and bottom steel). In such cases full depth cracks can exist in the beams at the column faces but it is anticipated that significant bond force from the beam bars will be transferred to the ends of the diagonal compression concrete strut.

With regard to vertical shear reinforcement, the intermediate column bars of Unit 3 and 4 provided 27% and 33% of the total vertical joint core shear. Hence it could be recommended for ductile structures that the vertical joint core shear to be resisted by the concrete mechanism be taken as

$$V_{cv} = 0.7 V_{jv} \quad (7)$$

and hence that sufficient vertical shear reinforcement should be present to resist

$$V_{sv} = 0.3 V_{jv} \quad (8)$$

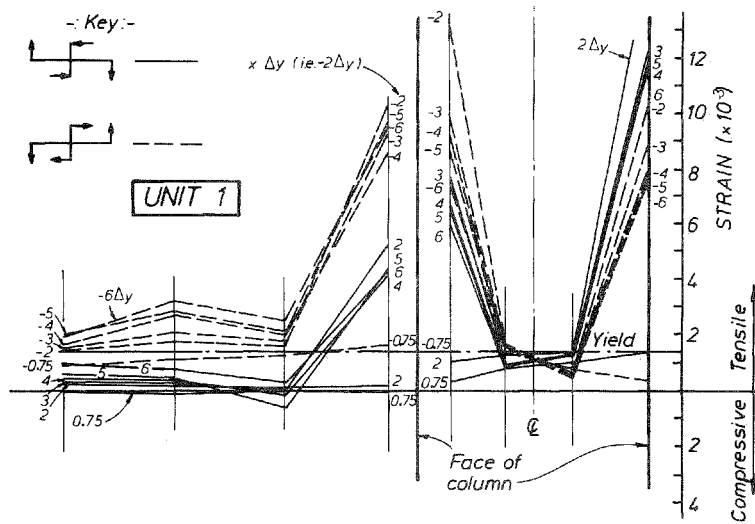
Note that NZS 3101 (2) at present permits $V_{cv} = 0.6 V_{jv}$ when $P_e = 0$ in symmetrically reinforced columns.

In frames of limited ductility lower levels of ductility are imposed. For example, a performance loading test could be four cycles of imposed loading to $\mu = \pm 3$. For frames of limited ductility with low axial load ($P_e \leq 0.1 f'_c A_g$) it could be recommended that

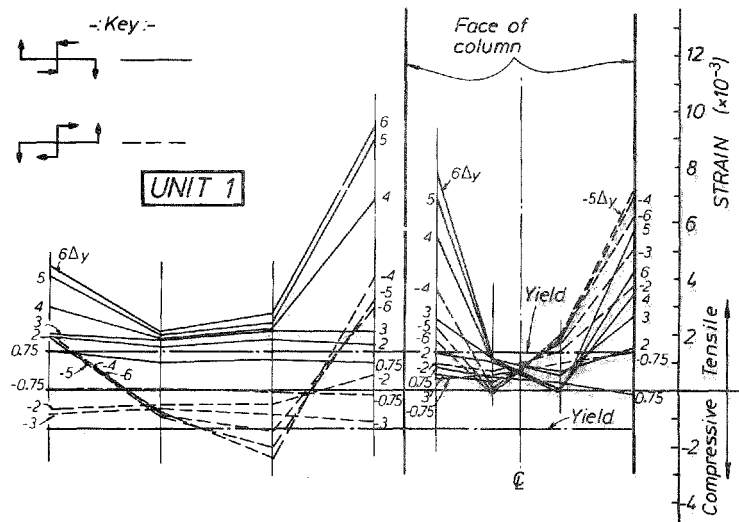
$$V_{ch} = 0.6 V_{jh} \quad (9)$$

and hence that

$$V_{sh} = 0.4 V_{jh} \quad (10)$$

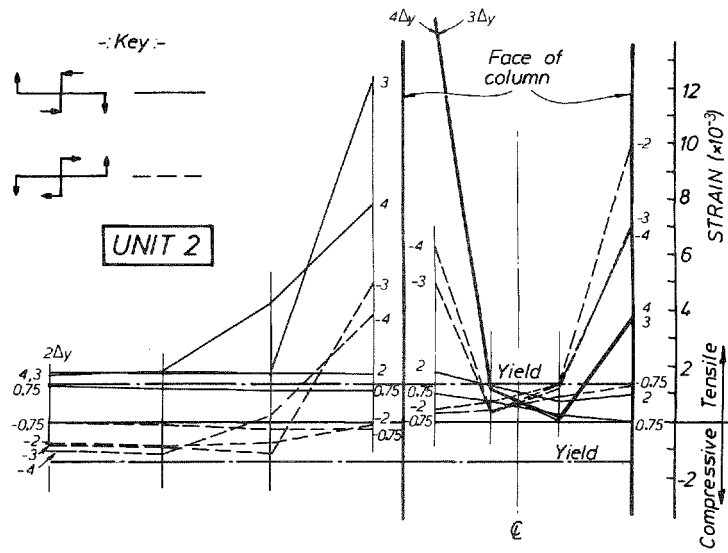


(i) Top bars

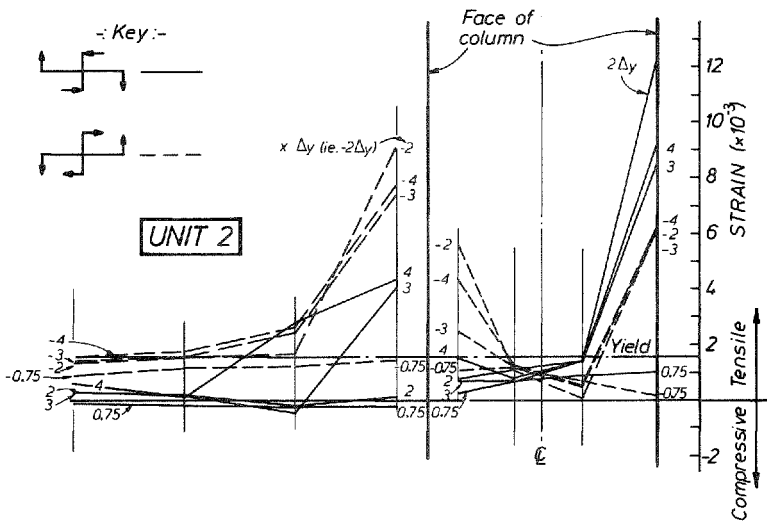


(ii) Bottom bars

Fig. 20(a) Strains Measured at Various Displacement Ductility Factor Levels on Longitudinal Beam Bars of Unit 1



(i) Top bars



(ii) Bottom bars

Fig. 20(b) Strains Measured at Various Displacement Ductility Factor Levels on Longitudinal Beam Bars of Unit 2

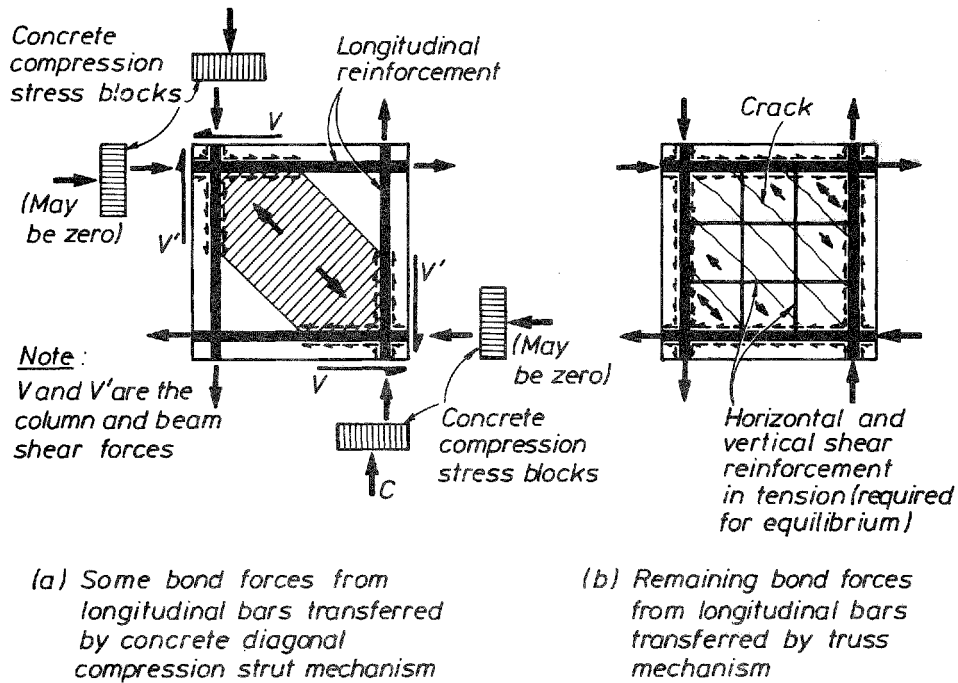


Fig. 21 Transfer of Bond Forces from Longitudinal Beam and Column Reinforcement Across a Beam-Interior Column Joint Core

and that at least one intermediate column bar exist at each side face of the column passing through the joint core.

For columns with higher axial load levels ($P_e > 0.1 f'_c A_c$) it is expected that the above V_e and g_v values given by Eqs. 5, 7 and ch_9 could cv be multiplied by a factor which is 1.0 for $P_e = 0$ and increases to greater than 1.0 as a function of $P_e/f'_c A_c$ as P_e increases. Such multiplying g factors e already exist in NZS 3101.

5.2 Development of Longitudinal Reinforcement Passing Through Beam-Column Joint Cores

The tests on Units 2 and 4 showed that the use of Grade 275 deformed longitudinal beam bars with a bar diameter to column depth ratio of 14.5, for beams when plastic hinges occurred at the column faces, was satisfactory. The maximum value for this ratio permitted by NZS 3101 for ductile frames is 1/25 for Grade 275 deformed steel.

It should be noted that the NZS 3101 requirement was determined to cater for the worst case when the concrete compressive strength f'_c can be as low as 20 MPa and where yielding of beam bars occurs in compression on one side of the column and in tension on the other side (see Fig. 22a).

In Units 2 and 4, f'_c was 36.0 and 40.1 MPa, respectively, and f'_c hence it could be expected that the bond strength of the concrete, which is a function of the square

root of f'_c (5), was significantly higher than for when $f'_c = 20$ MPa.

Also, when beams have equal top and bottom steel areas, full depth cracks form in the beams at the column faces during cyclic loading in the inelastic range, and since $C_s = T$ for equilibrium (see Fig. 22a) the compression steel must reach the yield strength. However when the top and bottom beam steel is unsymmetrical, with a greater area of steel in the top than in the bottom, it is evident that during cyclic loading in the inelastic range a full depth crack still develops during positive moment but the compression (top) steel cannot yield (see Fig. 22b). If $A'_s/A_s = 0.51$ as in Units 2 and 4 it is apparent that the compressive stress in the top steel will be approximately one half of the stress in bottom (tension) steel. Hence the bond stress requirements will be less demanding.

Assuming uniform bond stress u_b along the beam bars of diameter d_b in the joint core, and a column of depth h_c , the following equation can be written for a bar for the case of $A'_s = \beta A_s$, where $\beta \leq 1$.

$$\beta A_s \alpha f_y + A_s \alpha f_y = \pi d_b h_c u_b \quad (11)$$

where α is the beam steel overstrength factor.

$$\therefore (1 + \beta) \frac{\pi}{4} d_b^2 \alpha f_y = \pi d_b h_c u_b \quad (12)$$

Also, since the bond stress u_b is a function of the tensile strength f'_c of the concrete, $u_b = K \sqrt{f'_c}$ can be substituted into Eq. 12, where K is a constant and f'_c

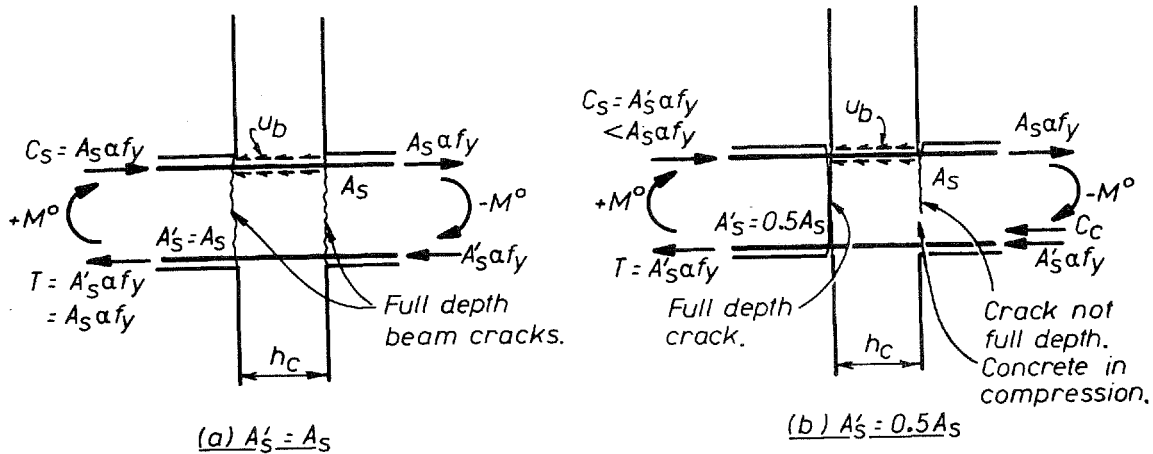


Fig. 22 Forces Acting on Beam Longitudinal Bars Across an Interior Joint Core

is the compressive strength of the concrete. Then

$$\frac{d_b}{h_c} = \frac{4K \sqrt{f'_c}}{(1+\beta) \alpha f_y} \quad (13)$$

For Units 2 and 4, on average $f'_c = 38.1$ MPa. Also, for the top bars $d_b/h_c = 1/14.5$, $\beta = 0.51$ and it can be assumed that $\alpha f_y = 1.25 \times 275 = 344$ MPa. Substituting these values into Eq. 13 it is found that $K = 1.45$.

As another method of calibrating Eq. 13, the NZS 3101 requirements of $d_b/h_c \leq 1/25$ for Grade 275 steel and $d_b/h_c \leq 1/35$ for Grade 380 steel can be used for the worst case when $f'_c = 20$ MPa and $\beta = 1.0$. Then for these NZS 3101 requirements and assuming $\alpha = 1.25$, $f'_c = 20$ MPa and $\beta = 1.0$, Eq. 13 gives $K = 1.54$ for Grade 275 steel and $K = 1.52$ for Grade 380 steel. These values for K are close to that obtained above for Units 2 and 4.

Substituting $K = 1.53$ and $\alpha = 1.25$ into Eq. 13 gives the following equation which could be recommended as a suitable code requirement for deformed longitudinal bars in the top of beams of ductile frames when the beam plastic hinges develop at the column faces:

$$\frac{d_b}{h_c} \leq \frac{4.9 \sqrt{f'_c}}{(1+\beta) f_y} \quad (14)$$

Equation 14 is for the case where the column axial compressive load level is low ($P_e \leq 0.1 f'_c A_g$). When columns have higher axial compressive load levels it is expected that the above d_b/h_c value could be multiplied by a factor which is greater than 1.0 which increases as $P_e/f'_c A_g$ increases.

For frames of limited ductility it would appear that no restriction on the d_b/h_c ratio is necessary.

6. JAPANESE AND UNITED STATES RECOMMENDATIONS FOR DEVELOPMENT OF LONGITUDINAL BEAM REINFORCEMENT IN JOINT CORES

Research at the University of Tokyo by Kitayama et al (10) has examined the inelastic dynamic response of 4, 7 and 16 storey moment resisting frames with the plastic hinge behaviour of the beams modelled by stiffness degrading hysteresis hoops with and without pinching behaviour caused by bond deterioration. The effect of significant pinching of the hysteresis hoops was found to be relatively small and it was concluded that some bond deterioration of beam bars within a beam-column joint may be tolerable. The University of Tokyo equation for the beam bar diameter limitation proposed by Kitayama et al (10), as a result of their assessment of experimental tests on reinforced concrete beam-column subassemblages and dynamic analyses, is

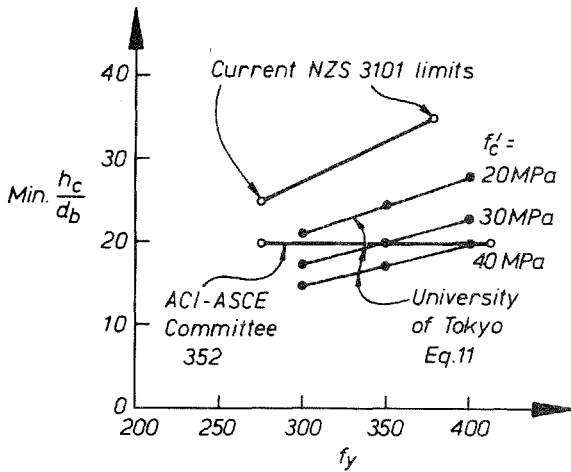
$$\frac{d_b}{h_c} \leq \frac{3.2 \sqrt{f'_c}}{f_y} \quad (15)$$

where f'_c and f_y are in MPa units.

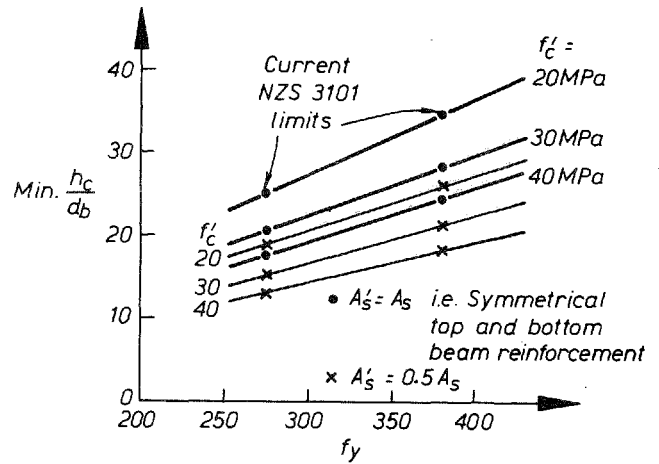
It is also of note that the most recent report of ACI-ASCE Committee 352 (11) has recommended that for beams $d_b/h_c \leq 1/20$.

The current New Zealand code requirements, the University of Tokyo Eq. 15, the ACI-ASCE Committee 352 recommendation, and the proposed Eq. 14 are shown plotted for comparison in Fig. 23.

It should be borne in mind that Japanese codes specify higher seismic design loads at the ultimate limit state than the New Zealand code, and hence a smaller available ductility is required of Japanese structures than for New Zealand ductile structures. Hence the larger diameter bars permitted by Eq. 15 are understandable.



(a) Comparison of NZS 3101, University of Tokyo and ACI-ASCE Committee 352 requirements



(b) Comparison of NZS 3101 and proposed requirements

Fig. 23 Comparison of Existing and Proposed Requirements for Ratio of Minimum Column Depth to Beam Bar Diameter Ratio

The proposed Eq. 14 agrees with the current NZS 3101 requirements when $f'_c = 20$ MPa and $\beta = 1.0$, but permits some relaxation of those requirements when $f'_c > 20$ MPa and/or when unsymmetrical beam steel arrangements are used ($\beta < 1.0$).

The extent to which inelastic shear and bond mechanisms should be permitted to participate in the hysteretic behaviour of a ductile moment resisting frame is still a controversial matter. Although some variations in hysteresis loop shape may not have a major influence on the inelastic dynamic response of structures subjected to major earthquake excitation, there is no doubt that it is much easier to repair the flexural damage occurring at well detailed plastic hinges in beams than to repair damage resulting from inelastic shear and bond mechanisms.

However it is believed that the current NZS 3101 provisions for beam bar diameters could be relaxed along the lines recommended in this paper.

6. CONCLUSIONS

1. The tests conducted on four beam-column Units, representing the joint region at interior columns of moment resisting frames, with plastic hinging occurring in the beams at the column faces, indicated that the current NZS 3101 requirements for the quantity of shear reinforcement in beam-column joint cores, and for the diameter of beam bars passing through the joint core, could be made less stringent.

2. The shear carried by the concrete diagonal compression strut mechanism across the joint core, which is commonly referred to as the shear resisted by the concrete, in two of the Units was higher

than that permitted by NZS 3101:1982. It is recommended as a result of analysis of the test results that:

- (a) For beam-interior column joints of ductile frames, if the column axial load level is low (less than $0.1 f'_c A_c$, where f'_c = concrete compressive cylinder strength and A_c = gross area of the column), and when plastic hinges form in the beams adjacent to the column faces, the horizontal joint core shear force resisted by the concrete be

$$V_{ch} = 0.4 V_{jh}$$

and hence that horizontal shear reinforcement should be present to resist

$$V_{sh} = 0.6 V_{jh}$$

and that the vertical joint core shear force resisted by the concrete be

$$V_{cv} = 0.7 V_{jv}$$

and hence that vertical shear reinforcement should be present to resist

$$V_{sv} = 0.3 V_{jv}$$

where V_{jh} = design horizontal joint core shear force and V_{jv} = design vertical joint core shear force.

The above equation for V_{ch} was obtained from beam-column Units with a ratio of beam longitudinal bottom steel area to top steel area of 0.4 to 0.5, but the equation is expected to be also adequate for cases with equal top and bottom steel.

(b) For beam-interior column joints of frames of limited ductility $V_{ch} = 0.6 V_{jh}$ and hence $V_{sh} = 0.4 V_{jh}$ may be assumed and at least one intermediate column bar should exist at each side face of the column passing through the joint core.

3. The diameter of the beam bars passing through the joint core in two of the Units was higher than is permitted by NZS 3101:1982. It is recommended as a result of analysis of the test results that:

(a) For interior beam-column joints of ductile frames, when plastic hinges form in the beams adjacent to the column faces, the diameter of deformed longitudinal bars in the top of beams passing through the joint core should satisfy

$$\frac{d_b}{h_c} \leq \frac{5 \sqrt{f_c}}{(1+\beta) f_y}$$

where d_b = bar diameter, h_c = column depth in the direction under consideration, and β = ratio of area of longitudinal bars in bottom of the beam to the area of longitudinal bars in the top of the beam, but β is not to exceed unity. For bottom beam bars the above equation for d_b/h_c may be used with β defined as the ratio of the area of top beam bars to the area of bottom beam bars, but β is not to exceed unity. The above equation for d_b/h_c was derived for columns with low axial compression load levels. It is likely that higher values for d_b/h_c could be permitted at higher axial compression load levels.

(b) For beam-interior column joints of frames of limited ductility no restriction of the d_b/h_c ratio is necessary.

ACKNOWLEDGEMENTS

The work described herein was conducted in the Department of Civil Engineering of the University of Canterbury, New Zealand, by Mr. Dai Ruitong, who is a Lecturer at the Branch College of Tongji University, Shanghai, China, during his stay at the University of Canterbury as a visitor under the supervision of Professor R. Park. The financial assistance provided by the University of Canterbury is gratefully acknowledged. Professor T. Paulay is thanked for his comments. Special thanks are due to technicians Messrs. G.W. Sim, N.J. Hickey, G.E. Hill, N.W. Prebble, H.H. Crowther, L.H. Gardner and Mrs. V.J. Grey and to secretary Mrs. J.Y. Johns.

REFERENCES

- "Code of Practice for General Structural Design and Design Loadings for Buildings, NZS 4203:1984", Standards Association of New Zealand, Wellington, 1984.
- "Code of Practice for the Design of Concrete Structures, NZS 3101 Part 1:1982", and "Commentary on the Design of Concrete Structures, NZS 3101 Part 2:1982", Standards Association of New Zealand, Wellington, 1982.
- Draft Replacement for "Code of Practice for General Structural Design and Design Loadings for Buildings, NZS 4203:1984", Standards Association of New Zealand, Wellington, 1986.
- "Structures of Limited Ductility, Report of a Study Group of NZNSEE", Bulletin of New Zealand National Society for Earthquake Engineering, Vol. 19, No. 4, Dec. 1986, pp.285-336.
- Park, R. and Paulay, T., "Reinforced Concrete Structures", John Wiley, New York, 1975, p.769.
- Paulay, T., Park, R. and Priestley, M.J.N., "Reinforced Concrete Beam-Column Joints Under Seismic Actions", Journal of the American Concrete Institute, Proceedings Vol. 75, No. 11, Nov. 1978, pp.585-593.
- Paulay, T. and Park, R., "Joints in Reinforced Concrete Frames Designed for Earthquake Resistance", Research Report 84-9, Department of Civil Engineering, University of Canterbury, June 1984, p.71.
- Dai Ruitong and Park, R., "A Comparison of the Behaviour of Reinforced Concrete Beam-Column Joints Designed for Ductility and Limited Ductility", Research Report 87-4, Department of Civil Engineering, University of Canterbury, June 1987, p.65.
- Andriono, T. and Park, R., "Seismic Design Considerations of the Properties of New Zealand Manufactured Reinforcing Bars", Bulletin of the New Zealand National Society for Earthquake Engineering, Vol. 19, No. 3, Sept. 1986, pp.213-246.
- Kitayama, K., Otani, S. and Aoyama, H., "Earthquake Resistant Design Criteria for Reinforced Concrete Interior Beam-Column Joints", Proceedings of Pacific Conference on Earthquake Engineering, Vol. 1, Wairakei, New Zealand, Aug. 1987, pp.315-326.
- ACI-ASCE Committee 352, "Recommendations for the Design of Beam-Column Joints in Monolithic Reinforced Concrete Structures", Journal of American Concrete Institute, Proc. V. 82, No. 3, March 1985, pp.266-283.